Department of Precision and Microsystems Engineering

Piezoelectric Energy Harvesting from Low-Frequency Vibrations

Marsha Nieuwland

Report no : 2021.086
Coach : T.W.A. Blad
Professor : P.G. Steeneken
Specialisation : MSD/DMN
Type of report : Master Thesis
Date : 11 November 2021

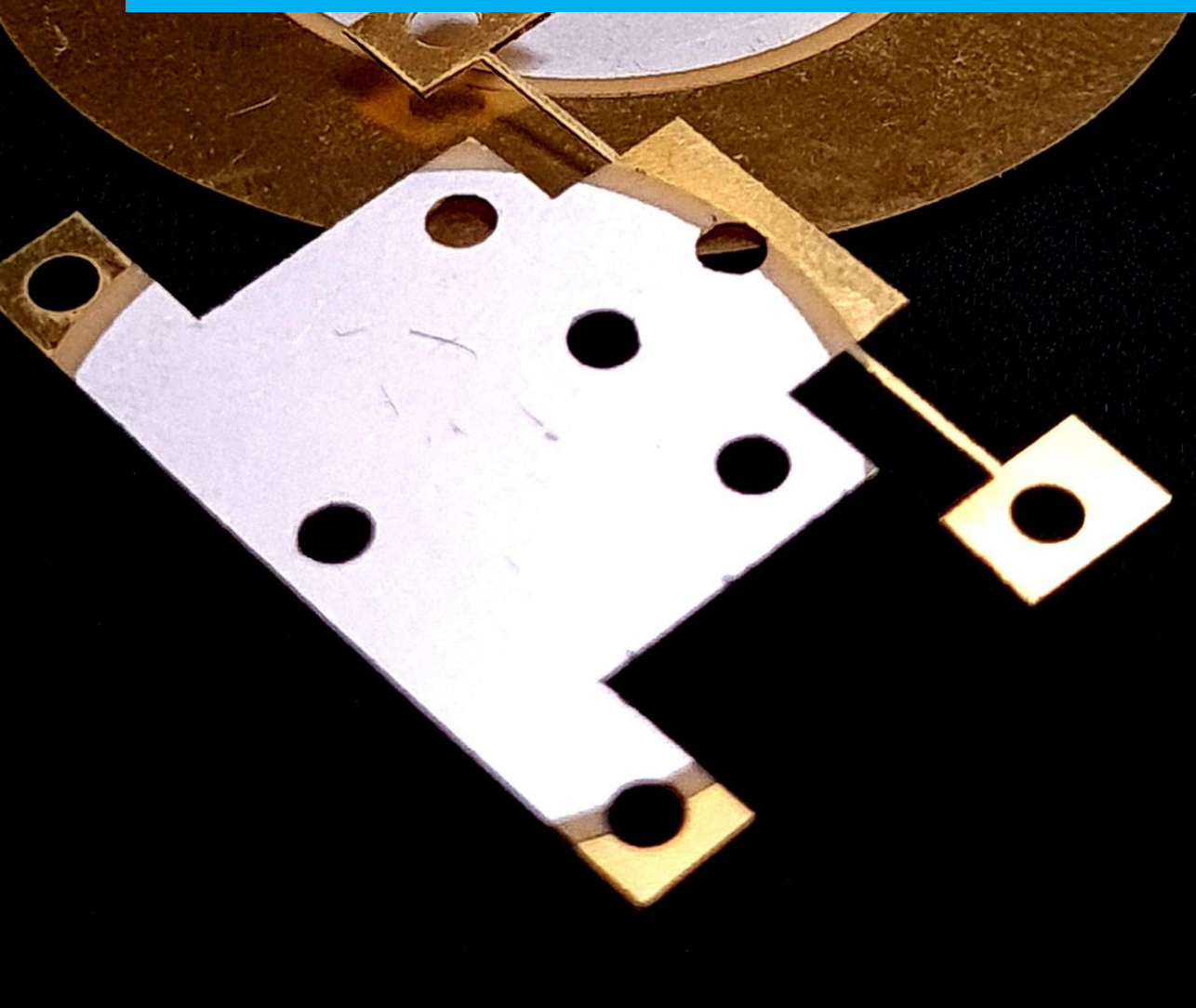

ENERGY HARVESTING FROM LOW-FREQUENCY VIBRATIONS

ENERGY HARVESTING FROM LOW-FREQUENCY VIBRATIONS

by

MARSHA NIEUWLAND

in partial fulfillment of the requirements for the degree of

Master of Science
in Mechanical Engineering

at the Delft University of Technology,
Department of Precision and Microsystems Engineering

to be defended on Thursday the 18th of November, 2021 at 14.00h.

Daily Supervisor:	Dr. Ir. T.W.A. Blad	TU Delft
Thesis Committee:	Prof. dr. P.G. Steeneken	TU Delft
	Dr. D.F. Machekposhti	TU Delft
	Dr. Ir. M. Wiertlewski	TU Delft

An electronic version of this thesis is available at http://repository.tudelft.nl/.

TU Delft Delft University of Technology

PREFACE

Solving puzzles and riddles was something I always liked to do when I was young. Soon, this resulted in passion for both math and physics, as to me all the question that were presented seemed to be one exciting big puzzle I had to solve. It was during those physics classes that I became enthusiastic about engineering. Seeing videos of the Tacoma bridge vibrating due to torsional flutter, made me realise that those questions on paper were actually applicable to real life situations. That is how I got excited for Mechanical Engineering, which in my opinion is a great combination of both the theoretical and practical side of engineering.

The clear societal benefits of energy harvesters, the high tech technology and the possible applications in the medical field made me enthusiastic about working on the vibration energy harvester technology for my graduation project. Even though vibration energy harvesting comes with its challenges, I am convinced that they can be overcome and that one day vibration energy harvesting will be widely used as a way to power low power medical devices.

Marsha Nieuwland
Delft, November 2021

CONTENTS

1

INTRODUCTION TO VIBRATION ENERGY HARVESTING

This chapter introduces the reader to the concept of vibration energy harvesting and discusses the challenges that come with it. The focus of the thesis is introduced and the general outline of the thesis is presented.

1

Energy harvesting is the principle of extracting energy from ambient sources and converting it into electrical power. Some well-known examples are solar panels, which harvest energy from light, and wind turbines, which harvest energy from the wind. Less known, yet also a very interesting source of energy, are vibrations. Even though vibrations are usually considered to be undesirable, the energy carried in those vibrations could potentially be used as useful power supply. The so-called vibration energy harvesters have been an interesting topic when it comes to the replacement of batteries in low-power devices.

1.1. VIBRATION ENERGY HARVESTING

Vibrations are everywhere: in your car as you drive over a speed bump, in railway trails caused by a passing train and even inside your own body in the form of your own heartbeat. Vibration energy harvesting is the practice of converting these vibrations into useful electrical energy. Especially with the increasing interest towards renewable energy sources, the research towards these energy harvesters has become increasingly more interesting.

Maybe one of the most interesting fields of application for vibration energy harvesting is the medical field [1]. As the power consumption of wearable and implantable devices has gone down, the use of vibration energy harvesters has become more interesting and meaningful. Think of hearing aids that can power themselves by the energy provided by human motion or a pacemaker of which the battery does not have to be replaced after several years because it is self-powering. The idea of using energy harvesters as an infinite power source, makes it an interesting research topic.

1.1.1. TRANSDUCERS

An important part of the energy harvesting process is the conversion from mechanical energy to electrical energy. Transducers are responsible for this conversion and can be categorized into three groups: electromagnetic, electrostatic and piezoelectric transducers. This has been depicted in Figure 1.1.

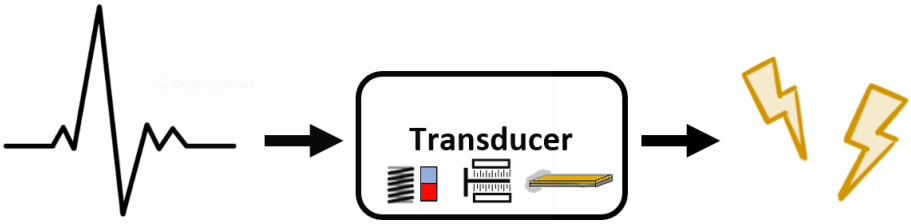

Figure 1.1: Schematic visualisation of the conversion from mechanical energy to electrical energy by means of a transducer.

The electromagnetic transduction principle is based on the relative movement of a conductor in a magnetic field, resulting in an induced voltage on the conductor. The most common example is a permanent magnet moving in a conductive coil. While on macro scale the use of induction can be very effective, this advantage is usually lost during miniaturization. Loss of magnet strength and limited space for coil loops makes for less efficient energy harvesting at small scale [2].

Electrostatic transducers make use of a relative motion between two pre-charged capacitor plates. This results in a varying capacitance because of which a voltage is induced. Fabrication methods for electrostatic MEMS devices are already in place, making them suitable for miniaturization. However, a drawback of electrostatic transducers is the initial voltage that is required to charge the capacitor in the first place, which impacts the efficiency of these type of transducers [2].

Piezoelectric transducers are made of materials that exhibit the piezoelectric effect: when undergoing mechanical stress, a voltage is induced due to the shifting of positive and negative charge centers in the molecule structure. Piezoelectric materials are known for their high power densities and ease of application [3], making it a very promising transduction method to be used in miniaturized vibration energy harvesters.

TRANSDUCTION METHOD OF CHOICE

For the reasons mentioned above, the piezoelectric transducers have shown to be the most promising when it comes to the application in miniaturized vibration energy harvester. Therefore, the focus of this thesis will be on vibration energy harvesters that make use of piezoelectric transducers

1.1.2. CHALLENGES

LOW-FREQUENCY AND LARGE-AMPLITUDE EXCITATION

Human motion usually consists of low frequencies and large motion amplitudes. However, the performance of most piezoelectric energy harvesters is relatively poor at these frequencies [4]. As most piezoelectric transducers are quite stiff, a large gap exists between the low operating frequencies and the relatively high natural frequency of the transducer. Especially with the current trend of miniaturization, high natural frequencies become even more of a problem. Therefore, making use of resonance at low frequency and small scale can be difficult. Especially when the amplitude of the motion is way larger than the device itself, the use of resonance becomes merely impossible[5].

AVAILABILITY PIEZOELECTRIC TRANSDUCERS

When it comes to the design of a piezoelectric transducer, the options are quite limited. The design of the energy harvester has to be adjusted to fit a standard off-the-shelf transducer or the transducer has to be custom made, which can become expensive. Because of this, the transducer becomes limiting to the design of the energy harvester.

TESTING METHODS

The performance of vibration energy harvesters are mostly evaluated by means of a frequency sweep performed by an electrodynamic shaker. These standard tests do not rep-

resent real life excitations well and might therefore give a distorted view of what is possible when it comes to virbation energy harvesting.

1.2. THESIS OUTLINE

In this thesis, a research is presented with a focus on energy harvesting from low-frequency vibrations. The specific case of energy harvesting for pacemakers is looked into in more detail. The research includes topics such as: frequency-up conversion, fabrication of piezoelectric transducers, stiffness compensation and energy harvesting for pacemakers.

A literature research is presented on impact-driven frequency up-converters in Chapter 2. The state of the art of this field of research is presented, followed up by a classification and an analysis in order to identify relations between their performances and specific design variables.

Chapter 3 focuses on the fabrication of piezoelectric transducers by modifying piezoelectric diaphragms, which are often used in audio buzzers. Different fabrication techniques are discussed that could be used to obtain more freedom when it comes to the design of the piezoelectric transducer.

In Chapter 4, a paper is presented with a focus on energy harvesting for pacemakers. A stiffness compensated energy harvester was manufactured and its dynamic behaviour and practical performance was studied when applied to an actual heartbeat. In order to standardize testing for pacemakers, a signal representing a simplified heartbeat is introduced. A significant increase of power output was measured when the prototype was compared to a reference device. The results also showed the importance of using real world signals for testing. Big differences were observed when comparing results when a real world signal was applied and when standard sine waves were used.

Chapter 5 includes a reflection of the author, the most important conclusions and recommendations for future research are mentioned.

Work that was performed, but did not make it to the main body of this thesis, are discussed in the Appendices. Appendix A discusses the different prototypes that were manufactured during the project. Appendix B shows the results of measurements that were performed to see whether the stiffness could successfully be tuned by means of a varying preload. Appendix C talks about an attempt that was made to obtain zero stiffness in order to obtain an extremely low resonance frequency. Appendix D discusses an experiment that was performed in order to determine the order of magnitude of load resistance that should be used for measurements. Appendix E shows a step-by-step plan for the assembly of the stiffness compensated energy harvesters and dynamic testing. Appendix F shows a piezoelectric composite sample that was fabricated for this graduation project. Appendix G includes the results of measurements that did not directly fit in this thesis, but were still relevant. In Appendix H, a design of a frequency up-converter is presented.

2

A CLASSIFICATION OF IMPACT-DRIVEN FREQUENCY UP-CONVERTERS

A literature research was conducted on impact-driven frequency up-converters. The concept of impact driven frequency up-converters is introduced and the state of the art is presented. A classification is proposed based on the type of coupling between the low frequency oscillator and high frequency oscillator. An analysis was performed to identify relations between performances and different design variables of prototypes presented in literature and to see whether there were any distinct differences between the proposed categories.

A classification of impact driven frequency up-converters

M. Nieuwland[1], **T. W. A. Blad**[1], **P. G. Steeneken** [1]

[1] Department of Precision and Microsystems Engineering, Delft University of Technology, 2628 CD Delft, The Netherlands.
Correspondence: marshanieuwland@hotmail.com

Abstract. Energy harvesting from human motion has been an interesting field of research when it comes to extending the life time of portable medical electronics. However, it comes with its difficulties due to the large amplitude and low frequency characteristics of human motion. Frequency up converters have been presented as a solution to this problem, which can be grouped into two categories: plucking type and impact type. Even though frequency up converters have been vastly researched over the past decade, no clear design strategy is available when it comes to the impact type frequency up converters. In this research, a classification based on the location of impact is proposed. The peak efficiency and bandwidth are used to evaluate the performances of the different devices. Additionally, the relation between the performances and design variables are shown. The results suggest a relation between the performance and the motion ratio of the device. An interesting trade-off is observed, where an increase of in motion ratio results in a higher efficiency at cost of bandwidth. It is also suggested that the frequency ratio is an important design variable in relation to the bandwidth.

2.1 Introduction

In the last decade, wireless and portable electronic devices and sensors have been a hot topic, especially in the medical field. These devices are reliant on batteries, which have limited power and usually dominate the overall size of the device [6]. Continuous replacing of these batteries is usually expensive and inconvenient. In an effort to extend the life time of such batteries without increasing their size, energy harvesting from ambient vibrations has been investigated over the last few decades. Especially since the power consumption of certain applications has decreased, researching vibration energy harvesting has become more interesting and meaningful.

An interesting field to investigate when it comes to energy harvesting from vibrations, is the usage of human motion. As most portable medical devices are worn on or inside the body, using the human body as a source of energy is very appealing. However, these motions are mostly defined by large amplitudes and low frequencies (<10 Hz) [7], which makes efficient energy harvesting difficult. This is because the energy harvester is usually smaller than the applied motion amplitude, making the use of resonance difficult or even impossible. To overcome this problem, frequency up converters (FupC) for energy harvesting have been vastly researched the past decade [8]. A FupC consists of a low frequency oscillator, that absorbs energy from the low frequency excitation. This low frequency oscillator than activates a high frequency oscillator, causing the low frequency excitation to be up conversed into a high frequency motion. Due to energy conservation, this frequency up conversion also results in a lower motion amplitude.

These FupCs have been categorized in different ways, for example according to their transduction type [9] and improvement aspect [8]. Blad and Tolou distinguished between FupC based on plucking and impact, in which the latter uses the impact of an impact member to excite a secondary oscillator. A variety

of impact based FupCs have been reported over the years. For example the design presented by Gu et al. [10], in which a driving beam representing the low frequency oscillator impacts a generating beam, the high frequency oscillator. Lots of variations of this design have been proposed, where the number of driving beams and generating beams vary[11][12][13]. Also completely different designs have been reported, for examples designs making use of snap-through behaviour of buckled bridges [5][14] and designs in which the low frequency oscillator and high frequency oscillator are connected in series, where the low frequency oscillator impacts a casing in order to obtain an impulse like response of the high frequency oscillator[4][15].

However, even though such a variety of designs have been proposed when it comes to impact based FupCs, no clear overview of the different systems have been presented. In addition to that, a method of comparing the FupCs and a clear overview of important design parameters have not been presented either. Therefore, no design strategy is available when it comes to designing FupC by means of impact.

The research objective of this literature review is to propose a classification in order to compare the impact based FupCs and to identify relations between the performances and different design variables of the FupCs.

In the first section "Method", the method is elaborated on, including the introduction of the metrics and design variables that are used throughout the paper. "Classification" introduces the classification and section "Results" presents the results per group, followed up by the section "Discussion" in which the results are interpreted and discussed. This is followed up by section "Recommendations" and section "Conclusion".

2.2 Method

This section introduces the different parameters and metrics that will be used to compare the performances of different FupCs.

2.2.1 Generator Figure of Merit

To compare the performances of different FupCs, a general way of performance evaluation is required. Mitcheson et al. [16] proposed the volume figure of merit FoM_V, by which the efficiency of different devices can be compared as a function of their overall size. In order to account for the geometry of the device as well, Blad et al. [5] proposed the generator figure of merit FoM_G (equation 2.1).

$$FoM_G = \frac{P_{avg}}{\frac{1}{16} Y_0 \rho_M V L_Z \omega^3} \times 100\% \tag{2.1}$$

With P_{avg} being the average power, the Y_0 motion amplitude, ρ_M the density of the proof mass, V the total volume of the generator and L_z The dimension of the generator along the direction of the applied motion. When Y_0 is not given, it can be calculated by using equation 2.2 in case of a harmonic function, with a being the acceleration and ω the frequency.

$$Y_0 = \frac{a}{\omega^2} \tag{2.2}$$

As the FoM_G represents a curve and can therefore not directly be used to compare the FupCs, the peak efficiency η_{peak} will be used as a way to compare the different systems, see figure 2.1.

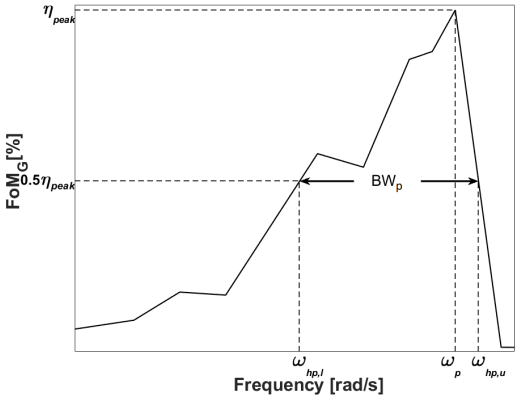

Figure 2.1: Example graph of the FoM_G plotted against frequency, with the peak efficiency η_{peak} and half efficiency bandwidth BW_{nhe} indicated.

2.2.2 Normalised half efficiency bandwidth

Most testing results were obtained by either a frequency (up) sweep or by applying different single-frequency excitations. Therefore, the bandwidth of these devices can be evaluated. To do so, the normalised half efficiency bandwidth is used, in which ω_p, $\omega_{hp,l}$ and $\omega_{hp,u}$ represent the frequency at peak efficiency, the lower bound at half of the peak efficiency and the upper bound at half of the peak efficiency respectively (see figure 2.1).

$$BW_{\text{nhe}} = \frac{BW_{\text{p}}}{\omega_{\text{p}}} = \frac{\omega_{\text{hp,u}} - \omega_{\text{hp,l}}}{\omega_{\text{p}}} \tag{2.3}$$

2.2.3 Design Parameters

Motion ratio

The dimension of the generator along the direction of the applied motion L_z has a significant influence on the efficiency of a generator. As the use of FupCs will most likely be applied in scenarios in which the generator is small compared to the applied motion, the motion ratio λ proposed by Blad et al. [5] is interesting to investigate. Comparing the motion range of the proof mass with the motion range of the driving motion, should give some information about the possible efficiency of a generator. The definition of the motion ratio is as follows.

$$\lambda = \frac{L_z}{2Y_0} \tag{2.4}$$

Mass ratio

The mass ratio is introduced in order to determine whether the choice of mass is of influence on the performance. The mass ratio is defined as below, with M_{HFO} the mass of the high frequency oscillator, M_{LFO} the mass of the low frequency and $M_{HFO,total}$ the total mass of all high frequency oscillators in case there are more. In case of a system described in section 2.3.1, M_{LFO} represents the mass of the moving mass.

$$\Psi = \frac{M_{HFO}}{M_{LFO} + M_{HFO,tot}} \tag{2.5}$$

Frequency ratio

In order to determine whether the natural frequency of the high frequency oscillator is an important design parameter, the frequency ratio is introduced. The frequency ratio is defined below, in which ω_{HFO} is the natural frequency of the high frequency oscillator and ω_p the frequency at peak efficiency.

$$\phi = \frac{\omega_{HFO}}{\omega_p} \tag{2.6}$$

2.3 Classification

In order to compare the different FupCs, a classification is proposed. The designs are classified based on the location of impact. This can take place between the base and the low frequency oscillator (LFO) and between the low frequency oscillator and high frequency oscillator (HFO). The FupCs in these groups are referred to as 'hammer type' and 'stacking type' respectively. A mass-spring-damper model of both groups can be found in figure 2.3a and figure 2.3b. An overview of the classification can be found in table 2.1.

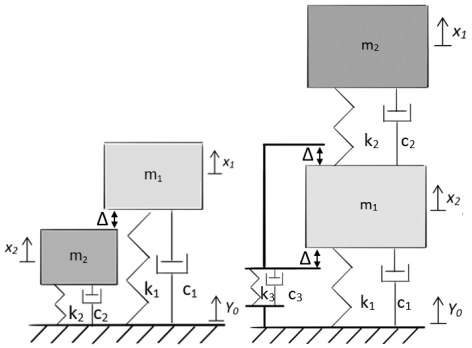

(a) I: Hammer Type (b) II: Stacking Type

Figure 2.3: Mass-spring-damper model of FupCs where the LFO and HFO impact each other (a) and of FupCs where the LFO impacts the base (b).

2.3.1 I: Hammer type

The first group consists of systems in which the low frequency oscillator impacts a high frequency oscillator. The following equation of motion can be found:

$$dz < \Delta$$

$$\begin{aligned} m_1\ddot{z}_1 + c_1\dot{z}_1 + k_1 z_1 &= m_1\omega^2 Y_0 \sin(\omega t) \\ m_2\ddot{z}_2 + c_2\dot{z}_2 + k_2 z_2 &= m_2\omega^2 Y_0 \sin(\omega t) \end{aligned} \tag{2.7}$$

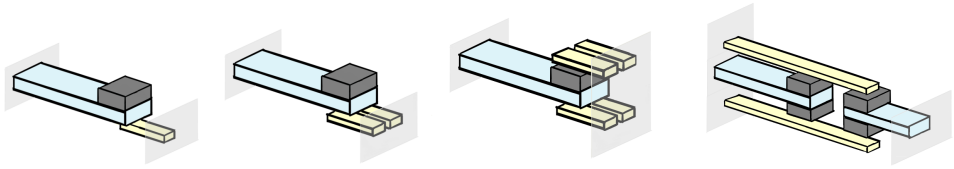

Figure 2.2: The different configurations of driving beams and generating beams reported of the hammer type group. Driving beams are colored blue, generating beams yellow and proof mass dark grey.

Class	Location of impact	Subcategory	Source
I	LFO-HFO (Hammer Type)	a. $k_1 > 0$	Halim et al. [7], Dauksevicius et al. [9][14], Gu et al. [6], Wang et al. [8]
		b. $k_1 = 0$	Renaud et al. [15], Halim et al. [16]
II	Base-LFO (Stacking Type)	a. $k_1 > 0$	Dechant et al. [11], Ashraf et al. [12]
		b. $k_1 < 0$	Blad et al. [17]

Table 2.1: Classification of the impact based FupCs.

$$dz \geq \Delta$$

$$\begin{aligned} Eq(2.7) + c_2\dot{z}_2 + k_2 z_2 &= m_1\omega^2 Y_0 \sin(\omega t) \\ Eq(2.7) + c_1\dot{z}_1 + k_1 z_1 &= m_2\omega^2 Y_0 \sin(\omega t) \end{aligned} \tag{2.8}$$

with $z_1 = x_1 - y_0$, $z_2 = x_2 - y_0$, $dz = x_2 - x_1$ and Eq (2.7) being the relevant left side of equation 2.7.

In the most simple case, a driving beam representing the LFO collides with a generating beam, causing the latter to vibrate freely. Examples of such devices are given by Gu et al.[10], Liu et al.[17] and Zorlu et al.[18]. Other show alternatives in which multiple driving beams and generator beams are used in order to increase the power density[11][12][13]. The different reported configurations of driving beams and generating beams can be seen in figure 2.2. Only Dauksevicius et al.[13] presented a system including multiple driving beams. It is claimed that when the natural frequency of both resonators are integer multiples of each other, both resonators constructively contribute to the amplification process during coupled vibration. Compared to the same FupC but with only one resonator, the result showed a 90% more power output on average. It must be noted, that this increase in power is obtained by adding more mass to the system. This makes it questionable whether the increase in power output is due to the design strategy or due to the increase of mass, or both.

A downside of the systems mentioned earlier, is that after fabrication the frequency range for which the system is suitable, is fixed. Lensvelt et al.[19] proposed a novel design in which both the low frequency oscillator and high frequency oscillator are configured to be electrostatic combs instead of cantilever beams. Clever use of out-of-plane gap-closing combs and interdigitated combs, makes for an adaptable natural frequency of the low frequency oscillator, as its stiffness becomes dependent on the input voltage ($k_{eff} \propto V^2$). Even though the results show no significantly large improvement of the bandwidth, it is an interesting idea to make use of an adaptable natural frequency even after fabrication. Such a device could potentially be used for active tuning. However, it is argued by Roundy et al. [20] that it is difficult or even impossible for active tuning

to produce more energy than it consumes.

Systems with $k_1 = 0$

The systems in the second category can again be split up into two groups: systems with a low frequency oscillator ($k_1 > 0$) and systems where the low frequency oscillator is replaced by a free sliding mass ($k_1 = 0$). Renaud et al. [21] came up with a detailed model of such a device, paying special attention to the dynamics of the impacting parts. The presence of so called secondary collisions is elaborated on, causing this type of systems to be difficult to model correctly, which is the case for almost all hammer type FupCs.

2.3.2 II: Stacking type

The second group consists of designs of which the location of impact is located between the base and the low frequency oscillator. The following equation of motion can be found:

$$|z_1| < \Delta$$

$$m_1\ddot{z_1} + c_1\dot{z_1} + k_1 z_1 - c_2\dot{z_2} - k_2 z_2 = m_1\omega^2 Y_0 \sin(\omega t)$$

$$m_2\ddot{dz} + c_2\dot{dz} + k_2 dz = m_2\omega^2 Y_0 \sin(\omega t) \tag{2.9}$$

$$|z_1| \geq \Delta$$

$$Eq(2.9) + c_3\dot{z_1} + k_3 z_1 - k_3\Delta = m\omega^2 Y_0 \sin(\omega t)$$
$$m_2\ddot{dz} + c_2\dot{dz} + k_2 dz = m_2\omega^2 Y_0 \sin(\omega t) \tag{2.10}$$

With Eq (2.9) being the relevant left side of equation 2.9. Such a design was presented by Liu et al. [22], who used two cantilever beams connected in series with a mechanical stopper. The main disadvantage of using cantilever beams is that if the deflection is too large, the cantilever can be destroyed. Dechant et al.[4] proposed a design in which no cantilever beams were incorporated, but instead used a diaphragm with a seismic mass positioned in the center. As the diaphragm holder collides with stoppers, the seismic mass gets an impulse like response and starts to vibrate in it's natural frequency.

In both devices mentioned, the low frequency oscillator and high frequency oscillator are connected in series. This means that throughout the motion, there is a coupling between the two masses. Ashraf et al.[15] mentions an interesting downside of such designs. When after impact the energy is pumped towards the high frequency oscillator, this energy flow might reverse and go back towards the low frequency oscillator. Ideally, to prevent this from happening, both oscillators should move in orthogonal direction from each other. In the design presented by Ashraf et al. [15] this was not physically possible, but managed to tilt the movement of the high frequency oscillator by 60 degrees

Systems with $k_1 < 0$

Also within this group, systems have been presented in which the low frequency oscillator is replaced, but in these cases only bi-stable systems have been reported ($k_1 < 0$). Both Jung and Yun [14] and Blad et al.[7] proposed such a bi-stable system. When the excitation applied exceeds a certain value, snap through behaviour can be observed where a rapid transition takes place between two stable equilibrium states. Due to the strong stiffening effect at the end of such a transition, the high frequency oscillator experiences an impulse and starts vibrating in its own natural frequency. What is interesting about these devices, is that the power output is dependent on the applied acceleration, instead on just the applied frequency. This makes these devices interesting, as such a device can be tuned in a way that the snapping of the buckled bridges happens at maximum acceleration, at which the most energy can be conversed.

2.4 Results

Table 2.1 presents the classification of the reported generators that were included in the analysis. Three reported FupCs of the stacking type were reported of which one is a bi-stable system. Seven FupCs of the hammer type group were reported, of which five resonating systems and two free sliding mass systems. In figures 2.4, 2.5, 2.6 and 2.7 the plots can be found of the peak efficiencies and bandwidth against the different design variables.

Almost all data that was presented of the

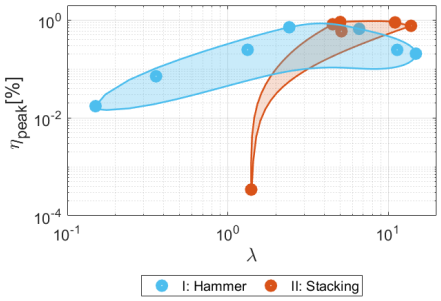

Figure 2.4: The peak efficiency plotted against the motion.

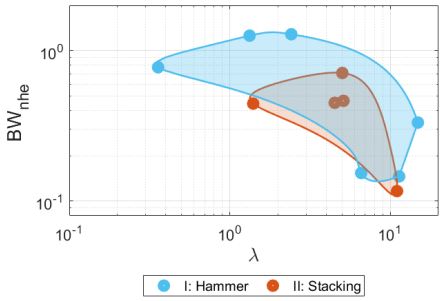

Figure 2.5: The normalized half efficiency bandwidth plotted against the motion ratio.

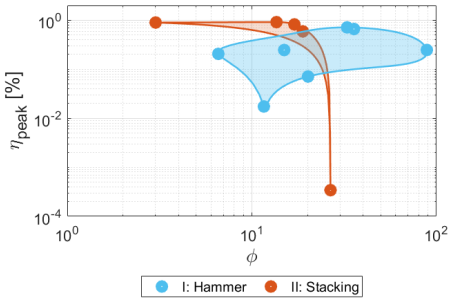

Figure 2.6: The peak efficiency plotted against the motion ratio.

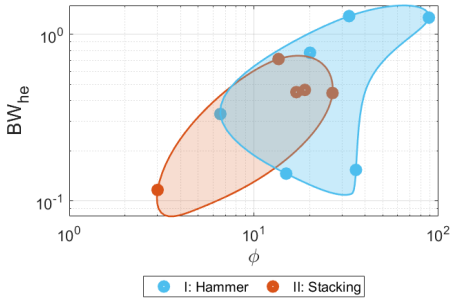

Figure 2.7: The normalized half efficiency bandwidth plotted against the frequency ratio.

power output were obtained by means of a frequency up sweep. Except for the data of the FupCs presented by Renaud et al.[21] and Halim et al.[23], these were tested by hand shaking. The input and output frequencies were in these cases determined by a Fast Fourier Transform (FFT) analysis.

2.4.1 Design Variables

For the hammer group, the reported motion ratios ranged from 0.15-14.89, the mass ratio ranged from 0.137-0.076 and the frequency ratio from 6.58-88.7.

For the stacking group, the reported motion ratios ranged from 1.40-13.9, the mass ratio ranged from 0.113-0.207 and the frequency ratio from 3.01-26.7.

2.4.2 Efficiency

Within the stacking group a range of FoM_G between 3.42e-4% and 0.91% was reported, whilst for the hammer group a range between 0.017% and 0.71% was found. Both the highest and lowest efficiencies that were reported were systems belonging to the stacking group: Blad et al.[24] with 3.42e-4% and Dechant et al. [4] with 0.91%. The two lowest reported efficiencies are both free sliding mass systems.

2.4.3 Bandwidth

Of the stacking type, a range of BW_{nhe} between 0.117 and 0.711 was reported, whilst for the hammer type a range between 0.146 and 1.286

was found. The highest half efficiency bandwidth was reported by Wang et al.[12] with 1.286 and the lowest by Ashraf et al. [15] with 0.117.

2.5 Discussion

A large variety of motion ratio, mass ratio and frequency ratio have been reported. However, when comparing the two groups, group stacking shows a smaller range of both motion ratio and mass ratio. This could be explained by the fact that only three different FupCs were reported. As seven FupCs were reported of group hammer, more variety can be expected when it comes to the design variables. This should be kept in mind when interpreting the results.

One explanation as to why that much more hammer type FupCs are reported than of the stacking type, might be because of the simplicity of the designs of the hammer type designs. The mentioned systems usually consist of cantilever beams which are relatively easy to fabricate, which might be a reason as to why more of these type designs are presented. However, the impacting dynamics are far from simple. Most models and experimental results differ, because of the assumption in the model that the impact is inelastic. In reality, this is not the case, as the coupled vibration includes multiple impacts[21] in practice which are not accounted for in the model, resulting in a lower power output than expected [10]. This makes correct modelling difficult or even impossible. This is not the case for the stacking systems, which is where the importance of the classification comes to play. When it is desired to focus on the influence of complex impacting dynamics or on designs which are easy to fabricate and adjust, FupCs of the hammer group might be the better the choice. When the focus lies within correctly modelling and predicting the FupC behaviour, stacking types might be the better choice. Performance wise, no group is preferred over the other.

In general, it can be noticed that the reported motion ratios were all quite large. This is probably because of the available testing devices and methods. The only two FupCs with a motion ratio lower than one were the once tested by shaking the device by hand. In these cases, a relatively large motion amplitude at a low frequency can be given as input. A regular shaker is not capable of providing large displacements, which is the most common testing device used for testing FupCs.

2.5.1 Efficiency

Most efficiencies reported of group stacking are relatively high comparing to the reported efficiencies of group hammer, even though the maximum reported efficiency of both groups are comparable. The hammer group shows a larger variety performance wise, which could be explained by the fact that more different devices were reported of this group.

When looking at figure 2.4, a trend can be observed of increasing peak efficiency with increasing motion ratio. The results of figure 2.5 suggest the opposite for the bandwidth, where the larger bandwidths are reported at lower motion ratios. Dechant et al. [4] showed that, while changing the gap between the stopper and the collision member, a higher efficiency could be achieved while decreasing its bandwidth and vice versa. This suggests indeed that increase of the motion ratio results in a higher efficiency, but at the cost of bandwidth. This could be an explanation as to why a couple of the systems show a relatively high efficiency, while showing a narrow bandwidth and the other way around. This trade-off between efficiency and bandwidth is interesting, with no clear 'right solution'. It would be interesting to investigate what balance of efficiency and bandwidth leads to the highest power output in real life applications. It must be noted that only few devices show such a clear difference between efficiency performance and bandwidth performance.

The stacking type systems show relatively large motion ratios, which could be a reason why these systems are relatively efficient compared to the other group.

No clear relationship was identified between the mass ratio and the peak efficiency. The same goes for the frequency ratio.

2.5.2 Bandwidth

Both groups show a large variety in bandwidth. Based on these results, no clear difference can

be identified between the half efficiency bandwidth of the two groups. What does seem to be of significant importance in relation to the bandwidth performance, is the frequency ratio. The results suggest that a large frequency ratio results in a large bandwidth. This could be an interesting design parameter. A relation between the bandwidth and the mass ratio was not found.

2.6 Recommendations

The proposed classification should be used early on in the design process. When the area of interest lies within complex impacting dynamics and easy fabrication, the hammer group might be the most interesting to look at. If the research direction goes more into obtaining a correct model that coincides with testing results, the stacking group might be more interesting to focus on.

When it comes to the test data, the average power, preferably obtained by a frequency sweep, should be given. This makes the comparison of different devices easier. The applied acceleration and the frequency at peak efficiency should be included as well.

In order to obtain more realistic data, different testing methods should be applied additionally. Frequency sweeps do not represent real life situations [25] and usually result in a motion ratio larger than one due to the available testing devices. The usage of FupCs is especially interesting in cases where the motion ratio is smaller than one. Therefore, testing methods which mimic human motion, including $\lambda < 1$ and irregular frequency patterns, will give more insights in the actual usability of the systems.

During the design process, special attention should be given to both the motion ratio and frequency ratio. Both design variables show a clear relation with the efficiency and bandwidth respectively and could therefore be of influence on the overall performance.

2.7 Conclusion

Even though frequency up-converters (FupCs) have been vastly researched over the past decade, no clear design strategy is available when it comes to the impact based FupCs. In this research, a classification based on the location of impact is proposed, which could be used as a tool during the design process in order to choose which type of impact-driven frequency up-converter might be most interesting in relation to the research objective. Through this classification, two type of impact-driven FupCs can be distinguished: the hammer type where the location of impact is between the low frequency oscillator and high frequency oscillator, and the stacking type, where the impact of location is between the base and the low frequency oscillator. To identify relations between the performances and different design variables, both the peak efficiency (η_{peak}) and normalized half efficiency bandwidth (BW_{nhe}) were derived for each device. The introduced design variables are the motion ratio (λ), mass ratio (ψ) and frequency ratio (ϕ).

A trade-off was observed, where devices show a large efficiency but narrow bandwidth and vice versa. The motion ratio seems to be of influence, as an increase of the motion ratio seems to result in an increase of efficiency, but a decrease in bandwidth. Furthermore, the frequency ratio showed to be of significant importance when it comes to the bandwidth, as a high frequency ratio is expected to result in larger bandwidth. No relation between the performance and mass ratio were observed.

The stacking group showed on average a higher efficiency than the hammer group, but their typical motion ratio was also found the be high. Only few motion ratios lower than one were reported, which is mostly because most tests were executed by means of a shaker. For future work, other testing methods resembling a human motion should be carried out as well to gain more insights of the performance of the devices in more practical situations.

3

THE FABRICATION OF PIEZOELECTRIC TRANSDUCERS

In this chapter, a fabrication method for piezoelectric transducers is presented in which piezoelectric diaphragms are modified in order to obtain a desired transducer design. Experiments were conducted to see whether micro laser cutting could successfully be applied to piezoelectric diaphragms in order to obtain a desired transducer shape. Additionally, milling and induced cracking was experimented with to see whether it would be possible to locally remove the piezoelectric layer from its substrate. An example of a piezoelectric transducer design that is made possible by the proposed fabrication method is presented.

3.1. INTRODUCTION

Piezoelectric transducers are popular in the field of energy harvesting. Usually, off-the-shelf transducers in the form of a cantilever or diaphragm are used in energy harvesters. When a more specific design is required, the transducer has to be custom made, which can become expensive. Often it is the case that the energy harvester design is adjusted in order to fit these standard off-the-shelf transducers. This is unfortunate, as the transducer than becomes leading in the design of the energy harvester, while it should serve the design of the energy harvester. Therefore, it is interesting to see what options there are to easily modify existing transducers to obtain a desired shape or design.

3.2. METHODS

3.2.1. PIEZOELECTRIC DIAPHRAGMS

An interesting type of piezoelectric off-the-shelf transducers to look into, are the piezoelectric diaphragms that can often be found in audio buzzers. The diaphragms consist of a circular metal substrate and a piezoelectric ceramic layer. The ceramic provides the energy harvesting capabilities, while the metal substrate provides support. Their simplicity and the fact that they are relatively cheap (<€1,-) makes them interesting for prototyping.

The piezoelectric diaphragms that were used for the experiments are the EPZ-20MS64W and KEPO FT-41T piezoelectric elements, which can be seen in Figure 3.1. Their dimensions are given in Table 3.1. The metal substrate is in both cases made of brass. Unfortunately, detailed information about the piezoelectric ceramic is missing. However, by visual inspection, it is thought that the piezoelectric ceramic is most likely lead zirconate titanate (PZT).

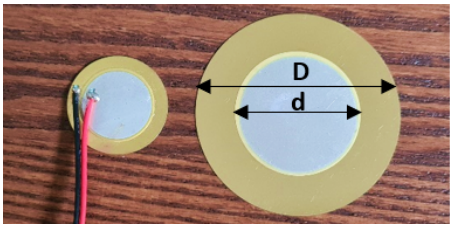

Figure 3.1: The EPZ-20MS64W and KEPO-41T piezoelectric diaphragms respectively.

Parameter	Symbol	EPZ-20MS64W	KEPO FT-41T
Outer diameter messing	D	20 mm	41 mm
Outer diameter piezoelectric ceramic	d	13.5 mm	25 mm
Layer thickness messing	t_m	0.2 mm	0.13 mm
Layer thickness piezoelectric ceramic	t_p	0.23 mm	0.10 mm
Total layer thickness	T	0.43 mm	0.23 mm

Table 3.1: An overview of the important dimensions of the piezoelectric diaphragms.

3.2.2. FABRICATION METHODS

LASER CUTTING

Mechanically cutting the diaphragms in order to obtain a certain shape would be an option, which should be done with a cutting mechanism that is able to cut through metal such as a tin snip or guillotine. However, this still limits the shapes that can be obtained. Therefore, instead of a mechanical cutting method, a thermal cutting method is looked into as this could potentially provide more flexibility and precision in the design of the transducer. In this case, laser cutting is the method of choice. Laser cutting is already successfully used as way to engrave piezoelectric diaphragms [26] and cut single layers of PZT [27] [28], which are in some cases bonded to a passive layer such as carbon fiber or sheet steel [29]. Laser cutting an off-the-shelf piezoelectric unimorph such as a piezoelectric diaphragm will make this bonding step unnecessary and will therefore speed up the fabrication process.

MILLING AND INDUCED CRACKING

In addition to laser cutting, milling and induced cracking are looked into as methods in order to locally remove the piezoelectric layer from the metal. This could open up the design space even more.

3.2.3. CURIE TEMPERATURE

The process of laser cutting consists of the removal of material through ablation of material that comes into contact with a focused laser. This could result in (local) high temperatures of the material, which if they exceed the Curie temperature of piezoelectric material, could badly affect the piezoelectric properties. It is interesting to see if laser cutting could successfully be used in order to modify piezoelectric diaphragms, or if the local high temperatures makes the use of this fabrication method inadequate. In all cases, unnecessary heat addition should be avoided.

3.2.4. TEST SET UP

LASER CUTTING

Experiments were performed to see if it was possible to cut through both the piezoelectric ceramic and the metal substrate by means of micro laser cutting. A Spectra-Physics Talon 355-15 DPSS UV laser system was used. The most important variables were determined to be the diode current I, laser speed v, laser frequency and the amount of passes N. Throughout the experiments a constant laser frequency of 50 kHz was used.

MILLING

During milling, the diaphragm was clamped to a piece of aluminum, which was clamped onto the milling machine (Emco FB4) which can be seen in Figure 3.2. The layer of ceramic was removed with a small cutter head (2-3 mm) on high speed (2500 rpm). The experiments were performed on both EPZ-20MS64W and KEPO FT-41T piezoelectric elements.

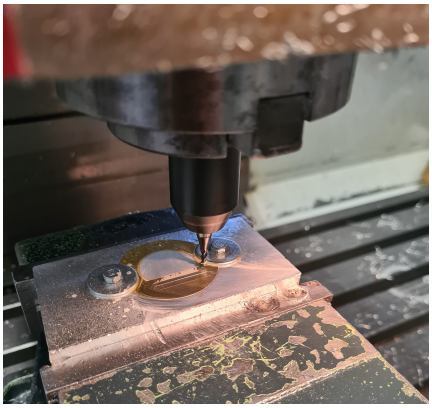

Figure 3.2: Milling of a piezoelectric audiobuzzer element

INDUCED CRACKING

For the induced cracking, again the Spectra-Physics Talon 355015 DPSS UV laser system was used, in combination with a sharp knife. Laser cutting was used to cut through the ceramic layer, isolating the material that was to be removed. The correct laser settings were determined during the experiment, which is elaborated on in section 3.4.1. After this, pressure was exerted on the isolated material using a sharp knife. Additionally, as an attempt to break the ceramic more easily, both star shaped an cross shaped cuts were added to the surface that had to be removed.

3.3. RESULTS: LASER CUTTING

3.3.1. EPZ-20MS64W

The first experiments were conducted using the EPZ-20MS64W piezoelectric element. The elements were placed with the piezoelectric side upwards, facing the laser, as can be seen in Figure 3.3. In order to cut through a material, it can be chosen to move the laser head relatively slow at low power, or, let the process run at high velocity but with high power. Because short run times were preferred due to the amount of experiments that were to be conducted, a relatively high speed and high power was used. The velocity and diode current were fixed during the experiment, being 150 mm/s and 7.5 A respectively. The number of passes was varied. Small circles with a diameter of 3 mm were cut multiple times for varying amounts of passes.

Table 3.2 and Figure 3.4 show the results for a different number of passes. An attempt was deemed successful when the shape was able to be removed from the surrounding material, no plastic deformation of the brass was visible and no continuity was present between the two conductive layers of the transducer. The latter was tested using a multimeter. If a continuity were to be present between the two conductive layers, the transducer would lose its energy harvesting capabilities.

As mentioned before, local high temperatures might influence the piezoelectric properties of the material. Therefore, the unnecessary addition of heat must be avoided, which is why the experiments were repeated until the minimum amount of passes that were required in order to successfully cut out the shape, was found. For the mentioned settings, this was about 1400 repetitions.

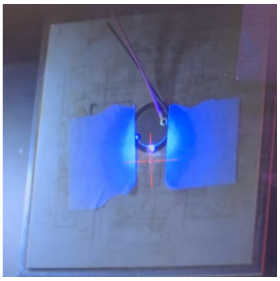

Figure 3.3: Laser cutting process.

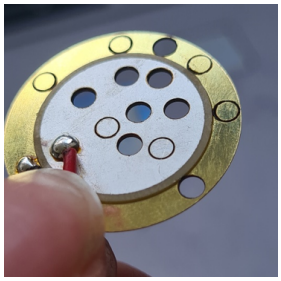

Figure 3.4: A EPZ-20MS64W element with successful and unsuccessful attempts.

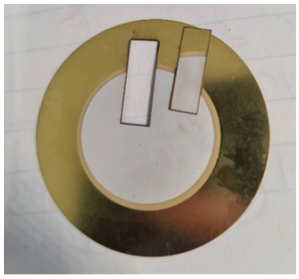

Figure 3.5: Rectangular geometry cut out of the KEPO FT-41T element

Passes (N)	Shape was removed from surrounding material	No plastic deformation of the brass layer was present	No continuity was present between the two conductive layers	Attempt was successful
2900	√	√	√	Yes
…	〃	〃	〃	〃
1400	√	√	√	Yes
1300	√	X	√	No
1150	X	-	-	No

Table 3.2: Results for varying passes for a set frequency of 50 kHz, diode current of 7.5 A and speed of 150 mm/s for the diaphragm with small diameter.

3.3.2. KEPO FT-41T

Because of the small diameter and relative large thickness of the EPZ-20MS64W element, another element was looked into as well. The KEPO FT-41T is larger and thinner compared to the EPZ-20MS64W, which could provide more design space when it comes to the design of the transducer and provides less stiffness than the other element. For the experiments conducted with the KEPO FT-41T elements, small cantilevers with a width of 5 mm and length of 15 mm were laser cut using a varying amount of passes, which can be seen in Figure 3.5. This new geometry allows for better visual inspection of the cut out shape. Again, the piezoelectric layer was placed upwards. The results can be seen in Table 3.3, showing that a minimum amount of 120 passes was required for a successful cut.

Passes (N)	Shape was removed from surrounding material	No plastic deformation of the brass layer was present	No continuity was present between the two conductive layers	Attempt was successful
150	√	√	√	Yes
120	"	"	"	"
100	√	X	√	No
80	X	-	-	No
70	X	-	-	No

Table 3.3: Results for varying passes at a set laser frequency of 50 kHz, diode current of 7.5 A and speed 150 mm/s.

One of the causes of a failed attempt, happened when the cantilever was almost completely cut through, but was still attached to surrounding material at a few points. If it was then attempted to release the shape by means of force, the geometry deformed before release. This is due to the ductile properties of the metal. To avoid this from happening, the element was flipped, so now the brass is faced upwards towards the laser. As the piezoelectric ceramic is way more brittle, it is expected that even when the laser has not entirely cut through both layers yet, it would be easier to release the shape by means of a bit of force. In Table 3.4 the results of both configurations can be seen. Only 80 passes were required for a successful attempt when the piezoelectric layer was faced downwards, while about 120 passes were required for a successful attempt when faced upwards.

Passes (N)	Successful attempt	
	Piezoelectric layer faced upwards	Piezoelectric layer faced downwards
150	Yes	Yes
120	Yes	Yes
100	No	Yes
80	No	Yes
70	No	No

Table 3.4: Comparison of the required passes for different orientations of the piezo.

3.3.3. SHORT-CIRCUITING ISSUES

In very few occasions, the two conductive layers would short circuit and the transducer would therefore lose its energy harvesting capabilities completely. This usually happened in cases where the element was burned quite badly as result of too many passes or when too much power was used during the process. It could be that very small particles of metal or silver ended up on the edge of the piece. As this only occured a few times, this was not looked into any further.

3.4. RESULTS: REMOVAL OF THE PIEZOELECTRIC LAYER

3.4.1. INDUCED CRACKING

Laser cutting was used in attempt to isolate parts of the ceramic, without cutting into the brass underneath. After this, the ceramic was attempted to be removed by using a sharp object to break the isolated ceramic. The correct settings of the micro laser cutting machine were determined experimentally. It is important to cut as deep as possible into the ceramic, without cutting in the brass layer. Circular patterns were laser cut for different settings, after which it was attempted to remove the ceramic by means of a sharp knife. For a diode current of 7.5 A and speed of 150 mm/s, it was determined by visual inspection that 850 passes seemed to show the least damage to the brass, while the ceramic was indeed removed.

Even though it was possible to locally remove the ceramic from the brass this way, the brass was damaged in all attempts. The pressure that had to be exerted in order to crack the ceramic was too high. As an attempt to make the ceramic crack more easily in order to not damage the brass when removing the ceramic, both star shaped and cross shaped cuts were engraved into the isolated part by means of laser cutting. The idea behind this is that these cuts might result in local stress concentrations, causing the ceramic to break more easily. For again a frequency of 50 kHz, diode current of 7.5 A, a speed of 150 mm/s, multiple cuts were made in the same circular shapes as mentioned above, using a varying amount of passes.

In Figure 3.6 the different steps that were taken can be seen. In all of the attempts, a dent was still present in the brass. What is interesting, is that more residue was left on the underlying brass in cases of a sample with a cross shaped cut and star shaped cut in comparison to the plain circles. This made the removal of the ceramic more difficult. It could be that because of the heat, the bonding between the ceramic and the metal actually becomes greater than without the additional heat. This could also be why the star shaped cut had even more residue left when comparing to the cross shaped cut, as more heat is added during the development of the star shaped cut than of the cross shaped cut.

Figure 3.6: Depiction of the the different patterns that were laser cut, the induced cracking and the resulting damage of the brass.

3.4.2. MILLING

In Figure 3.7 and Figure 3.9 two examples can be seen in which milling was successfully used as a way to remove the piezoelectric ceramic from the brass layer. Up milling made for a rough surface finish, while down milling resulted in a smooth finish (see Figure 3.9). The modified piezoelectric diaphragms did not lose their energy harvesting capabilities, therefore it can be concluded that this way of modifying piezoelectric diaphragms can successfully be used to separate the piezoelectric layer from the brass layer.

Figure 3.7: Ceramic removed in a single pass.

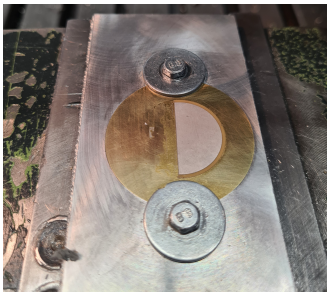

Figure 3.8: Ceramic removed after multiple passes.

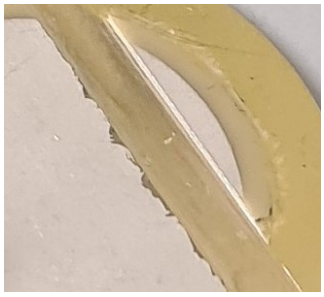

Figure 3.9: Close up showing the different finishes as a result of up milling (left side) and down milling (right side).

3.5. PROTOTYPING USING LASER CUTTING AND MILLING

To give an idea of what is possible when it comes to transducer designs by using the methods that were deemed successful, an example is given of an energy harvester which transducer was fabricated by means of laser cutting and milling. The prototype is an energy harvester in which negative stiffness is added to a piezoelectric cantilever by means of buckled flexures in order to lower its stiffness. This principle is mentioned in [30] and is elaborated on in the paper presented in Chapter 4 and Appendix A. As it might reduce assembly errors, it is desired to fabricate both the piezoelectric cantilever and buckled flexures out of one piece.

Because the flexures have to be flexible, they have to be ceramic free. Therefore, a combination of both micro laser cutting and milling was used to fabricate this part.The smallest feature of this transducer was the width of the two flexures. Even these small flexures with a width of 0.35 mm were easy to fabricate using micro laser cutting. The resulting transducer can be seen in Figure 3.10a and the assembled energy harvester can be seen in Figure 3.10b. Other examples that were used for prototyping can be found in Appendix A.

When the voltage output was measured over a 100 kOhm load when the mass was being moved by hand, a voltage output of 10 Volts was easily obtained. This showed that the transducer did not lose its energy harvesting capabilities.

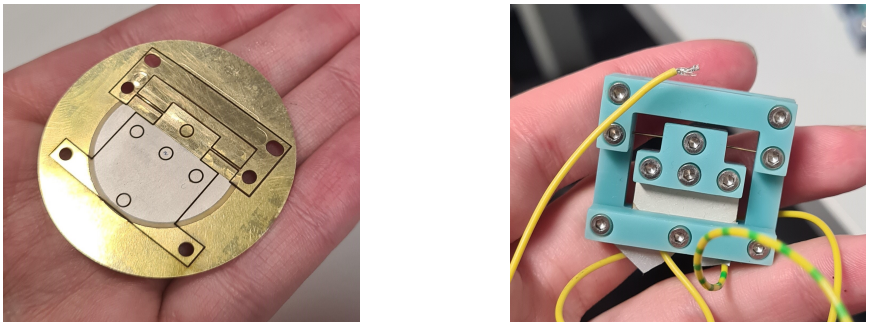

(a) (b)

Figure 3.10: a) Flexures-transducer combination as result of milling and laser cutting of a piezoelectric diaphragm. b) Assembled energy harvester.

3.6. CONCLUSIONS AND RECOMMENDATIONS

It can be concluded that both micro laser cutting and milling piezoelectric diaphragms are effective fabrication methods for the fabrication of piezoelectric transducers. For micro laser cutting, high speed and high power is preferred over low speed and low power. First cutting through the metal is preferred over first cutting through the ceramic, as this results in less required heat addition. Unnecessary heat addition must be avoided during the laser cutting process in order avoid short circuiting issues, which is something that occurred in very few occasions.

For milling, high speed downward milling is preferred in order to obtain a smooth surface finish. Also, a precision of at least 0.01 mm is desired, as the minimum layer thickness of the piezoelectric diaphragms that were used was 0.1 mm. Attempts of separating the two layers by means of induced cracking were unsuccessful, as they resulted in damage of the brass layer.

4

Stiffness Compensated Bistable Compliant Energy Harvester for Low- Frequency Operation tested on a Human Heartbeat

Paper

In this paper, a research is presented in which the dynamic behaviour and practical performance of a stiffness compensated bistable energy harvester is studied in relation to a human heartbeat. A prototype was build and tested on a motion stage. The results show a significant power output in comparison to a reference device.

Article

Stiffness Compensated Bistable Compliant Energy Harvester for Low-Frequency Operation tested on a Human Heartbeat

M. Nieuwland[1], **T. W. A. Blad**[1], **P. G. Steeneken** [1]

[1] Department of Precision and Microsystems Engineering, Delft University of Technology, 2628 CD Delft, The Netherlands.
Correspondence: marshanieuwland@hotmail.com

Abstract. In this work, the dynamic behaviour and practical performance of a stiffness compensated bistable energy harvester is studied when applied to a human heartbeat. The fabricated prototype consists of buckled flexures that are attached to a piezoelectric cantilever in order to provide negative stiffness. Because a human heartbeat is unique and is therefore difficult to replicate, a sawtooth wave was introduced to serve as a simplified human heartbeat in order to standardize testing for energy harvesting from the human heart. In comparison to a reference device, the power output was increased by a factor 14 and 1.3 for a sawtooth wave and amplified heartbeat respectively. When applied to a sine wave at the low frequency of 1.1 Hz and 1g, the power output was increased by a factor 57. This shows that stiffness compensated bistable energy harvesters are promising when it comes to the application in pacemakers and for low-frequency operation in general.

Keywords: Vibration energy harvesting; piezoelectricity; compliant mechanisms; pacemaker.

4.1 Introduction

In the last decades, vibration energy harvesters have been proposed as a solution to increase the lifetime of wireless and portable medical devices. As the power consumption of these devices has decreased, the application of vibration energy harvesters have become more interesting. One example of an implantable medical device for which energy harvesters could be interesting, are pacemakers. With a lifespan of about 6 to 12 years, the battery must be replaced surgically after this period of time [31]. Using an energy harvester instead of a battery is therefore seen as an interesting alternative.

The human heart rate is usually between 0.6-2Hz [32] and consists of low acceleration peaks (<1g). Miniaturization is required for the implementation of an energy harvester in a pacemaker. Because miniaturization comes with increased natural frequencies, this usually results in poor output power at low frequencies [33]. Especially when the amplitude of the applied motion is larger than the device itself, making use of resonance becomes even harder [5]. A bistable system could offer a solution, as the operability of these systems depend on excitation force instead of frequency. This makes them suitable for wideband operation, including low-frequency excitation [34].

Piezoelectric energy harvesters are most interesting to consider because of their miniaturization capabilities and high power densities of the piezoelectric transducer [35]. Cottone et al. [36] looked into energy harvesting by the buckling of a piezoelectric bimorph. It was concluded that the bistable buckled bimorph performed up to an order of magnitude better than the unbuckled bimorph. This concept was applied to a leadless pacemaker in the form of an analytical study

performed by Ansari and Karami [37]. It is shown that for a heartbeat acceleration signal with a peak acceleration of about 1.5g, a significant output could be generated. Jung and Yun [14] and Ando et al. [38] proposed a frequency up converter in which not the transducer itself is buckled, but is instead stacked upon a bistable mechanism. At the end of the snap through motion of the buckled mechanism, the transducers stacked upon the proof mass experience an impact to which they start to resonate in their natural frequency. In both cases it is shown that a wide operational-frequency range is obtained.

However, it is also mentioned that large threshold accelerations seem to be limiting to the use of bistable energy harvester, making them unsuitable for the application in pacemakers. Piezoelectric materials are known to be stiff, so buckling the piezoelectric transducer itself will most likely result in high required excitation forces to allow for snap through behaviour of the proof mass. Even when separating the buckling mechanism from the transducer, large threshold accelerations were still mentioned to be a problem [14]. In order to obtain a wideband bistable energy harvester operable for low-force excitation as well, stiffness compensation is required. The existing bistable energy harvester designs that include stiffness compensation, are mostly reliant on magnetic attraction and repulsion [39] [40] [41]. Even though they have shown promising results when it comes to wideband energy harvesting, the addition of magnets to a pacemaker makes the pacemaker incompatible for MRI scans [42]. Blad et al. [30] presented a magnetic-free stiffness compensated energy harvester where buckled flexures were used to provide negative stiffness to a relatively stiff piezoelectric cantilever, resulting in a sixfold increase in performance in comparison to a reference device.

Stiffness compensated bistable mechanisms show much potential when it comes to wideband energy harvesting. However, the performance of these energy harvesters is rarely tested under real world excitations.

The research objective of this paper is to study the dynamic behaviour and practical performance of an energy harvester with stiffness compensation under a real world excitation in order to bridge the gap between the standard lab tests and real world applications. The energy harvester consists of buckled flexures attached to a piezoelectric cantilever in order to provide negative stiffness to counteract the restoring force of the piezoelectric cantilever. The energy harvester is tested on an actual heartbeat signal which is magnified five times. In addition to that, a sawtooth acceleration signal is introduced to serve as a simplified heartbeat in order to standardize testing for energy harvesters that are designed to harvest energy from the human heart.

In Section 2 the design, the method of stiffness compensation by added buckled flexures, the fabrication process and test setup are elaborated on. In Section 3 the results of both the quasi-static measurements and dynamic measurements are presented and discussed. The conclusion can be found in Section 4.

4.2 Methods

4.2.1 Mechanical Design

The design of the stiffness compensated bistable energy harvester (SCOBIE) consists of a piezoelectric cantilever, a mass and flexures similar to the mechanism described in [30] (Figure 4.1). Furthermore, the prototype consists of a base and pre-loading blocks that can be set by means of a set screw, clamping parts and guidance pins to avoid rotation of the blocks, as used in [43]. The SCOBIE was assembled by sandwiching the flexure and cantilever between the mass. In addition to this mass, two metal rings were screwed onto this mass, resulting in a total proof mass m_p. The piezoelectric cantilever is fixed to the base and the ends of the flexures are fixed to the two preloading blocks. The preload displacement dL_f can be varied by tightening/loosening the set screw that connects the pre-loading block with the base. The gap between the base and preloading blocks is filled with a varying amount of spacers made out of 0.05 mm and 0.1 mm sheet steel.

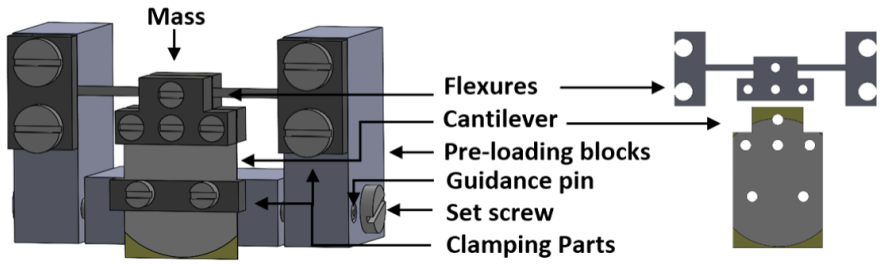

Figure 4.1: An overview of the energy harvester an its components, without the additional two mass rings that were attached to the plastic mass.

4.2.2 Stiffness Compensation

When a cantilever is forced out of its stable equilibrium position, a restoring force acts on the cantilever to bring it back to stability (Figure 4.2). In order to obtain a stiffness compensated mechanical design, a force has to be introduced that counteracts this restoring force of the relatively stiff piezoelectric cantilever. Therefore, preloaded flexures are added to the cantilever. Due to the preloading, the flexures will buckle out of plane and therefore apply a force to the cantilever in that same direction (Figure 4.2). When this force is designed to be equal to the restoring force of the piezoelectric cantilever beam, the design will be statically balanced over a certain range. When this force differs slightly in magnitude with respect to the restoring force of the cantilever, a low stiffness bistable system can be obtained.

This is visualized in Figure 4.3. When the buckled flexures are connected to the proof mass at the end of the cantilever, the resultant force will be equal to the sum of both devices separately. Both the negative stiffness provided by the buckled flexures and positive stiffness provided by the cantilever should nearly match in order to obtain the desired characteristics. The preload of the flexures can then be varied to tune the negative stiffness as well.

Figure 4.2: Visualization of the restoring force acting on the cantilever (on the left) and the out of plane force as a result of buckled flexures (on the right).

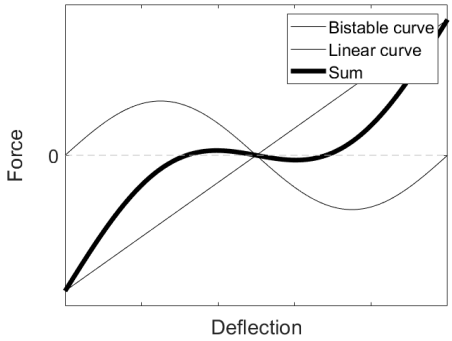

Figure 4.3: Resulting force- deflection curve by combining the monostable cantilever with the bistable flexures. The resulting curve is equal to the sum of the stiffnesses of both the linear cantilever and the bistable flexures.

4.2.3 Fabrication

Both the cantilever and flexures were laser cut using a micro laser cutting machine consisting of a Spectra-Physics Talon 355-15 DPSS UV laser system. The cantilever with length L_c and width w_c was fabricated by laser cutting a KEPO FT-41T piezoelectric diaphragm, consisting of a layer of brass and a layer of piezoelectric ceramic. The flexure with length L_f and width w_f was laser cut out of 0.1 mm sheet steel. The dimensions of the energy harvester are listed in Table 4.1 together with the settings that were used to laser cut the cantilever and flexure. The mass was 3d printed using a SLA machine (PRUSA SL1).

Parameter	**Symbol**	**Value**	
SCOBIE			
Flexure Length	L_f	11 mm	
Flexure Width	w_f	1.4 mm	
Preload Displacement Left/ Right	dL_f	0.58 mm / 0.74 mm	
Reference device & SCOBIE			
Cantilever Length	L_c	5.5 mm	
Cantilever Width	w_c	17.5 mm	
Thickness of the layer of brass	t_b	0.1 mm	
Thickness of the layer of piezoelectric ceramic	t_p	0.13 mm	
Mass	m_p	12.0 g	
Laser cutting		**Piezoelectric diaphragm**	**0.1 mm sheet steel**
Frequency	f	50 kHz	50 kHz
Diode current	I	7.5 A	7.0 A
Speed	v	150 mm/s	150 mm/s
Passes	N	150	100

Table 4.1: Relevant design parameters and laser cutting settings.

4.2.4 Test Set Up

All tests were performed for both the SCOBIE and a reference device. The reference device consists of only the monostable piezoelectric cantilever with the same proof mass attached to it as for the SCOBIE. No negative stiffness was added to the reference device.

Quasi static force- deflection measurements were performed using a PI M-505 motion stage, on which a FUTEK LRM200 sensor was mounted. The SCOBIE and reference device were mounted on a construction in front of the motion stage and were connected to the force sensor by means of a magnet (Figure 4.4a). The encoder embedded in the motion stage measures the displacement over which the stage is actuated, while the force sensor measures the reaction forces that are present during actuation.

The dynamic performance of the energy harvester was tested and measured using a linear motion stage (Figure 4.4b). Both the prototype and a reference device were mounted on the stage. The output was measured over a 200kOhm load.

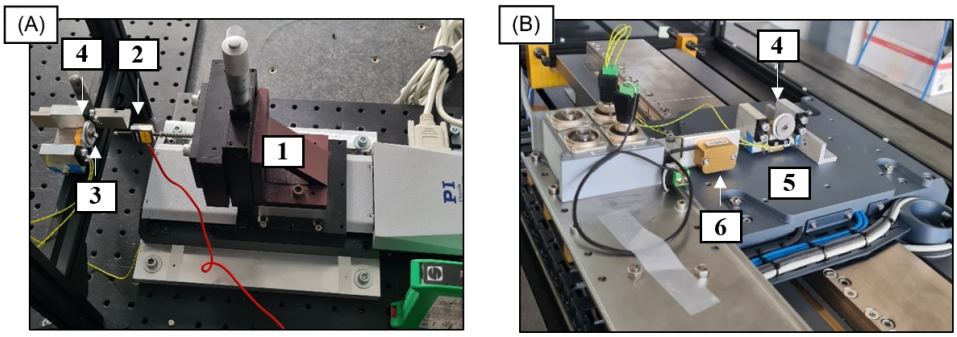

Figure 4.4: a) Test setup for quasi-static measurements consisting of a motion stage (1), force sensor (2), magnet (3) and the SCOBIE (4). b) Test setup for dynamical measurements consisting the SCOBIE (4), a linear motion stage (5) and accelerometer (6

4.2.5 Input Signals

A heartbeat consists of multiple frequencies layered on top of each other and lots of short acceleration spikes. To gain insight into a realistic performance of the energy harvester, it should be subjected to an actual heartbeat. Therefore, the energy harvester was subjected to a heartbeat of 120 bpm which was amplified five times in reference to the original signal (Figure 4.5a). The heartbeat signal was generated by combining three different sources of heart signals: open-chest acceleration measurements of pig hearts, ultrasound heart measurements of human hearts and human chest motions [44].

However, it must be noted that every heartbeat is unique. When heartbeats are used in scientific papers, they most likely differ as they are obtained from different sources and are difficult to replicate. This makes it difficult to compare the performances of prototypes presented in different scientific papers. Therefore, a signal is introduced that mimics the characteristics of a heartbeat, in a simplified and reproducible form: a sawtooth wave (Figure 4.5b). This signal consists of multiple frequencies and includes sudden changes in acceleration as well. It is expected that this signal will give a more realistic insight into the performance of the SCOBIE than the regular frequency sweep.

In order to get a more general understanding of the performance and behaviour of the SCOBIE, both devices were also subjected to an acceleration sweep from 0 to 2g at 2 Hz and the power was measured for a range of sine waves ranging from 1 to 10 Hz. The measurements of the sine waves

were performed over a period of 20 seconds, at constant frequency and acceleration. These measurements were performed twice: one at an acceleration which was sufficient enough to enable snap through behaviour of the SCOBIE and one at which this did not occur. This was determined to be 1g and 0.35g respectively.

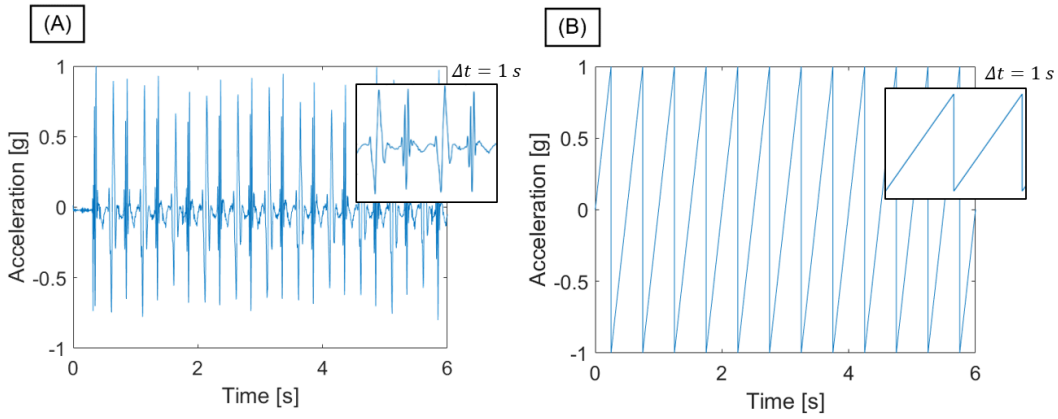

Figure 4.5: a) Acceleration profile of a heartbeat of 120 bpm (2 Hz) amplified five times. b) Acceleration profile of a sawtooth wave at 2 Hz and 1g.

4.3 Results and Discussion

4.3.1 Force- Deflection

In Figure 4.6 the results of the quasi static force- deflection measurements of both the SCOBIE and the reference device can be seen. The stiffness of the piezoelectric cantilever K_c is determined to be 850 N/m. When looking at the force- deflection curve of the prototype, it can be seen that a maximum of about 0.05 Newton has to be overcome in order for the mass to snap out of its equilibrium position towards the other equilibrium position. The travelled distance of the mass when snapping from one equilibrium position to the other is about 1.5 mm.

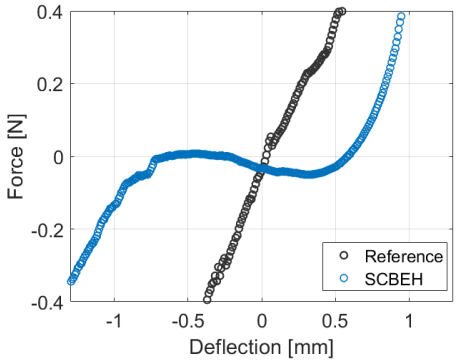

Figure 4.6: Measured force-deflection curve of the SCOBIE and reference device. The results show a range of motion of the SCOBIE of about 1.5 mm between the two stable positions, with a maximum force measured of 0.05 N within that range. The mono stable reference device shows a stiffness of about 850 N/m.

4.3.2 Acceleration Sweep

The results of an acceleration sweep from 0.1g to 2g at 2 Hz of both the reference device and the prototype are shown in Figure 4.7a and 4.7b. The SCOBIE starts to show snap-through behaviour starting at 0.4g, resulting in a drastic increase in voltage output. Accelerations lower than this limit, do not show any notable power output, as the mass stays in one configuration. The reference device without the flexures shows a gradual increase with increased acceleration. For accelerations lower than 0.4g, both devices show a similar voltage output. After 0.4g, the prototype outperforms the reference device.

When comparing the quasi-static measurements with the acceleration sweep measurements, it can be noticed that from both measurements the same conclusions can be drawn when it comes the required threshold acceleration for which the SCOBIE will show snap through behaviour. The quasi static force deflection measurements show that the force that is required to make the mass snap from one equilibrium point to the other one lies somewhere around 0.05 N. By Newton's second law, for a mass of 12 gram, this force is reached at an acceleration of 0.4g, which is shown to be the switching point at which the device starts to show snap through behavior.

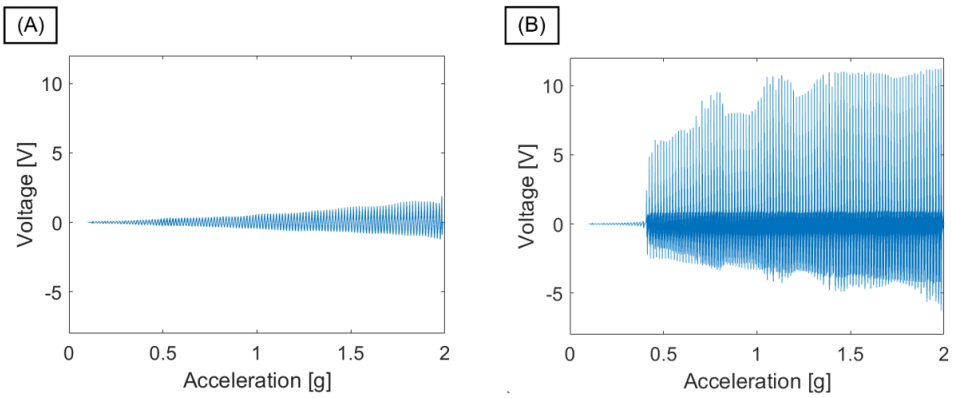

Figure 4.7: a) The results of an acceleration sweep where the acceleration was swept from 0.1 g to 2g over 60 seconds at 2 Hz. a) Voltage output of the reference device. b) Voltage output of the SCOBIE.

4.3.3 Frequency Response

Sine waves with frequencies ranging from 1 – 10 Hz for 0.35g and 1g were applied to both devices and their power outputs were measured. In Figure 4.8 the results of these measurements can be seen at 0.35g and 1g respectively. For the measurements performed at 0.35g, both devices show similar outputs. For measurements performed at 1g, the SCOBIE outperforms the reference device for the entire range of frequencies. At 1g and 1.1 Hz, the SCOBIE performs about 57 times better than the reference device (Figure 4.9).

The ratio between the power output of the reference device and SCOBIE can be seen in Figure 4.10 for both 1g and 0.35g. For sine waves at 1g, the results show a drastic improvement of power output over the entire range of 1-10 Hz. It can be seen that SCOBIEs are indeed interesting for wideband energy harvesting and especially for low frequency excitation. It can be expected that as the excitation frequency comes closer to the natural frequency of the reference device, the smaller the benefits of bistability will be compared to the reference device. However, at micro scale it is

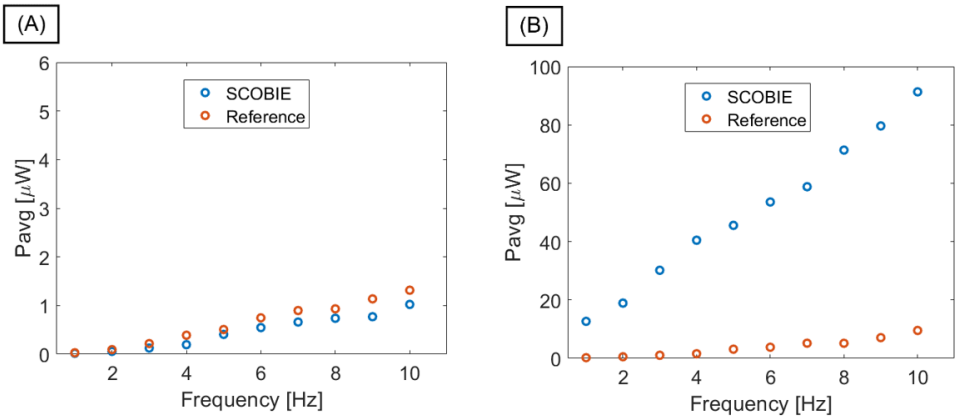

Figure 4.8: a) Test setup for quasi-static measurements consisting of a motion stage (1), force sensor (2), magnet (3) and the SCOBIE (4). b) Test setup for dynamical measurements consisting the SCOBIE (4), a linear motion stage (5) and accelerometer (6).

expected that the benefits of the SCOBIE will be even more profound. The natural frequency of the reference device will increase, resulting in a larger gap between the resonance frequency of the reference device and operating frequency and thus a lower efficiency is expected. When snap through motion is not occurring, which is the case for an acceleration of 0.35g, the reference device outperforms the SCOBIE. In this case the inertial force acting on the mass as a result of the applied acceleration is not high enough to overcome the potential energy barrier.

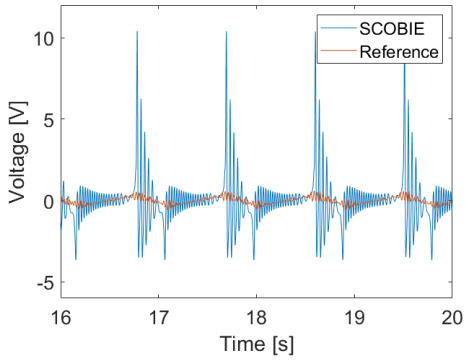

Figure 4.9: The voltage output of the SCOBIE and reference device at 1.1 Hz and 1g. The power is increased by a factor 57 when comparing the SCOBIE to the reference device.

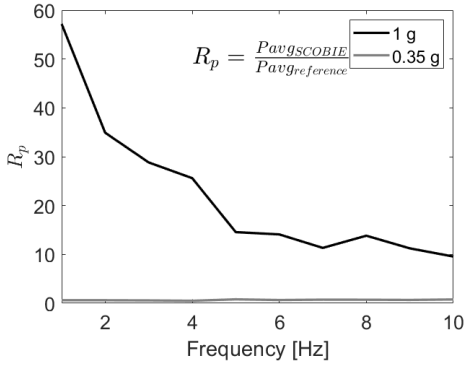

Figure 4.10: The power ratio for a frequency range from 1 to 10 Hz at 1g and 0.35g.

4.3.4 Sawtooth Wave and Heartbeat

The voltage outputs for the sawtooth wave at 2 Hz of both the reference device and the SCOBIE can be seen in Figure 4.11a and 4.11b. The average power output of the reference device was determined to be 2.4 µW, while the SCOBIE shows an average power output of 35 µW, which equals to about a fourteenfold increase in power output. The voltage outputs for the amplified heartbeat at 2 Hz of both devices can be seen in Figure 4.12a and 4.12b. The average power output of the reference device was 10 µW, while that of the prototype was 13 µW, which is an increase of about 30%. In both cases, the SCOBIE outperformed the reference device.

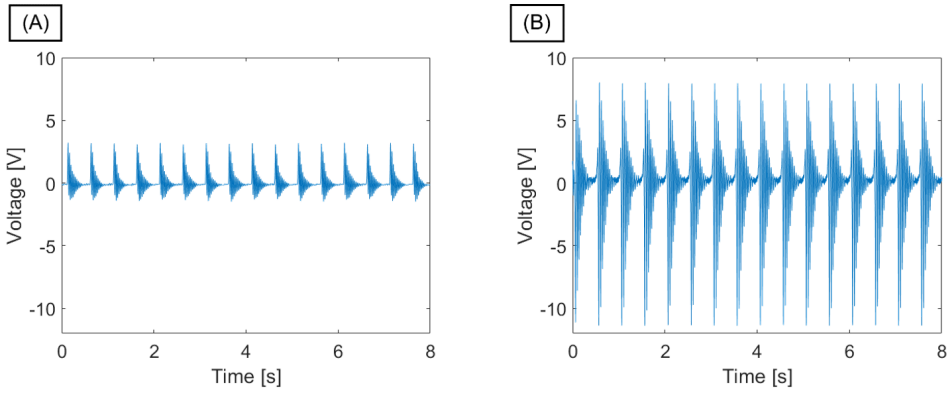

Figure 4.11: Voltage output for a sawtooth wave at approximately 2 Hz and 1g of a) the reference device and b) the SCOBIE.

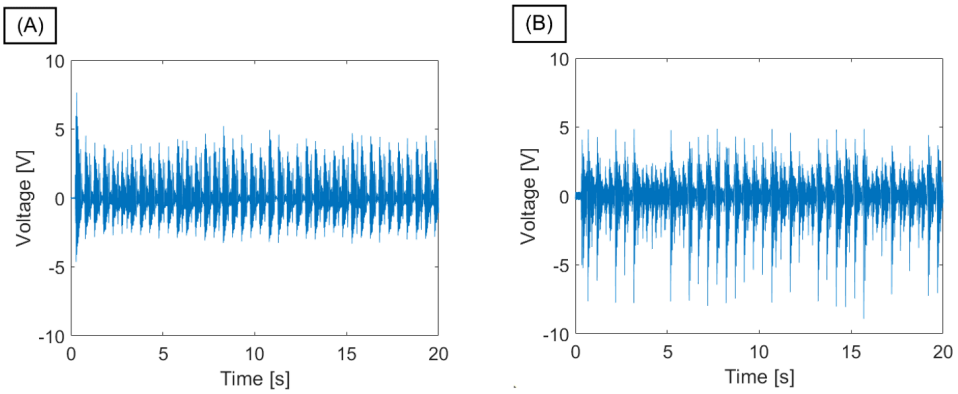

Figure 4.12: Voltage output for a heartbeat which was amplified five time wave at 120 bpm (2 Hz) of a) the reference device and b) the SCOBIE.

Sawtooth Wave

While sine waves consist of gradual changes in acceleration, a sawtooth wave includes a more sharp change in acceleration. For a sine wave, the SCOBIE switches from bistable point twice during one period. Two ring-downs can be observed in the voltage output, each is initiated during each snap through motion (Figure 4.13a). The input motion, input acceleration and voltage output

of the SCOBIE when applied to a sawtooth wave can be seen in Figure 4.13b. It was observed that the mass first snap through motion, indicated as I in Figure 4.13b, occurs relatively slow. As a sufficient acceleration is obtained, the mass slowly falls backwards relative to the acceleration. Shortly after that, the acceleration changes direction very abruptly, indicated as II in Figure 4.13, causing the mass to snap out of its equilibrium again and fall forward, but this time it happens very quickly and you can see the mass vibrate in its stable position afterwards. Because of the slow velocity obtained by the mass during the first snap through motion, this does not result in noticeable change in measured voltage output. Therefore only one ring-down is observed per period, while for a sine wave two ring-downs can be observed.

While for a 2 Hz sine wave the power ratio is about 35, for the 2 Hz sawtooth wave this is reduced to 15. The sudden acceleration change results in an impact like response of the mass, causing the reference device to resonate in its natural frequency of about 30 Hz. This ring-down that occurs carries a relatively high power density, resulting in a higher power output than expected. For the bistable energy harvester, this difference is not as pronounced, because in both cases the mass snaps from one stability point to the other, resulting in the same large displacements.

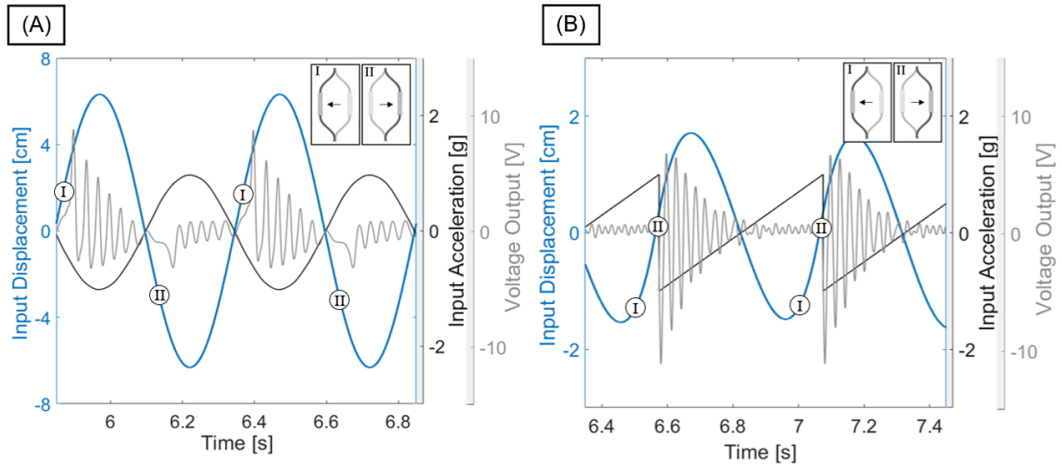

Figure 4.13: The input displacement, input acceleration and voltage output of the SCOBIE with the locations where the mass snaps out of equilibrium noted by I and II for a) a sine wave at 2 Hz, 1g and b) a sawtooth wave at 2 Hz, 1g.

Heartbeat

For the heartbeat at 2 Hz, the power ratio has been lowered to 1.3. The amplificated heartbeat signal consists of accelerations near zero, interchanged with quickly shifting acceleration peaks. This could explain why this again results in a higher power output of the reference device than expected. Also, acceleration peaks lower than 0.4g are present in the signal, which causes an increase in voltage output for the reference device in these moments. However, these acceleration peaks are not sufficiently high enough for the proof mass of the SCOBIE to snap out of its stable position, resulting in no large increases in voltage output in these moments. This shows the importance of lowering the threshold acceleration in order for energy harvesters to perform well when applied to a pacemaker. However, for the larger acceleration peaks, snap through behaviour is present. This results in a great increase in voltage output in these moments, which are the voltage peaks observed in Figure 4.12b.

Ideally, you want the threshold acceleration of the SCOBIE to match the maximum acceleration of the smallest acceleration spikes present in the heartbeat. This way the SCOBIE will show snap through behaviour at every spike in the acceleration signal and the snapping will happen at maximum acceleration, which is the moment in time the most power is present in the system and thus the most power can be generated. Threshold accelerations lower than the actual required acceleration will also result in snap through behaviour, but will also result in less efficient energy harvesting.

4.3.5 Efficiency

The performance of the SCOBIE at the frequency of 1.1 Hz and 1g is compared to other prototypes that were tested at low motion ratios and low accelerations that were presented in prior art in Table 4.2. The motion ratio λ (equation 4.1) is used to gain insight into the size of the generator relative to the amplitude of the applied excitation. The generator figure of merit FoM_G (equation 4.2) is used to compare the efficiencies of the different prototypes. With a volume of 50x30x30 mm and L_z of 30 mm, a motion ratio of $\lambda = 0.073$ and efficiency of 0.06% was found for a harmonic excitation at 1.1Hz and 1g.

Especially for energy harvesters with a motion ratio lower than one, this is already a significant efficiency. The dimension L_z of the SCOBIE is currently unnecessary large. Removing redundant volume in that direction will decrease the motion ratio (L_z) and increase the efficiency ($\propto L_z^{-2}$), without changing the power output. The presented efficiency is therefore an indication of what is possible, already showing a significant output for a relatively low motion ratio.

$$\lambda = \frac{L_z}{2Y_0} \tag{4.1}$$

$$FoM_G = \frac{P_{\text{avg}}}{\frac{1}{16} Y_0 \rho_M V L_z \omega^3} \times 100\% \tag{4.2}$$

Source	Vibration	Output Power	Motion Ratio	Efficiency
This work	1.1Hz, 1g	13.4 μW	0.073	0.06%
[30]	0.9Hz, 0.75g	55.6 μW	0.033	0.27%
[45]	0.25Hz, 0.28g	370 μW	0.063	1.00%
[21]	1Hz, 1g	47 μW	0.070	0.18%

Table 4.2: Comparison of the SCOBIE to other prototypes presented in literature.

4.3.6 Recommendations

The results show promising improvements in power output for the SCOBIE in comparison to the reference device. The next step would be to get the SCOBIE to work for threshold accelerations as high as that of the original heartbeat (<0.4g). For this design, the assembly by human hand and added up tolerances of the different parts made it challenging to easily tune the stiffness in order to lower the force that is required to obtain snap through motion. The resulting stiffness is quite sensitive to changes in the preloading displacement, so small errors or changes during assembly can have a significant effect on the performance of SCOBIE. A way to reduce assembly errors, would be to combine the flexures and cantilever into one part. This could be done by locally removing the piezoelectric layer of the piezoelectric element by means of milling in order to make space for the flexures, followed up by laser cutting the entire piece at once.

Also, an interesting next step is to look into actual miniaturization of the device. Because

miniaturization comes with increasing natural frequencies, it is expected that the performance of the resonant reference device will deteriorate when scaled down. It would be interesting to see what happens to the power ratio after miniaturization. However, before that could be tested, the design should be changed for it to be able to be fabricated at small scale. For example, the use of screws and the assembly of different parts with the human hand is impossible at miniaturized scale. Because of this, different ways of providing preload should be considered. An interesting approach specific for energy harvesters that could be applied to pacemakers is given by M. H. Ansari and M. Karami [37]. It is suggested to assemble a beam attached with both ends to a frame at relatively high temperatures compared to the operating temperature (body temperature). The mismatch of coefficients of thermal expansion between the beam and frame causes the beam to buckle when undergoing temperature changes relative to the temperature at which it was assembled. An interesting approach with the focus on actual implementation in the human body. Another approach is presented by the so called Package-Induced Preloading presented by Mariello et al. [46], where buckling is induced by laminating mechanisms that have been fabricated on the same substrate together with a frame over a geometry extending out-of-plane, shortening the in plane distance of the mechanism. This approach has already been demonstrated on small scale, making it an interesting concept that could be applied to miniaturized energy harvesters for pacemakers.

4.4 Conclusion

In this work the dynamic behaviour and practical performance of a stiffness compensated bistable energy harvester was studied under a real world excitation in the form of a heartbeat. The prototype consists of two buckled flexures and a piezoelectric cantilever to obtain snap through motion for low excitation forces. A variable preload displacement made tuning of the stiffness possible, resulting in a required force of 0.05 N for the mass to snap through from one stable position towards the other. This was validated by both force-deflection measurements and dynamic measurements.

A linear stage was used to measure the power output over a range from 1 to 10 Hz at 1g, showing a great increase in power output in reference to the monostable piezoelectric cantilever without the added negative stiffness. Measurements performed at the low frequency of 1 Hz showed an increase in average power output by a factor of 57 compared to the reference device. This shows that mechanically stiffness compensated bistable systems can be used in order to make energy harvesting for low force and low frequency excitations possible.

A sawtooth wave was introduced to mimic the characteristics of a heartbeat, in a simplified and reproducible form. For a sawtooth wave at 2 Hz and maximum acceleration of 1g, the prototype outperformed the reference device by a factor 15 when it comes to average power output. The energy harvester was also tested on an actual heartbeat that was amplified five times. In this case, the energy harvester showed increase by a factor of 1.3 in comparison to the reference device.

The results show a clear difference between the performance of the prototype when a sine was applied to the system and when a real world excitations was used. This shows the importance of using real world signals instead of the standard signals that are commonly used in lab tests.

5

REFLECTION, RECOMMENDATIONS AND CONCLUSIONS

This chapter includes the reflection of the writer, the most important conclusions of the presented research and recommendations for future research and more general recommendations.

5.1. REFLECTION

At the start of my graduation project, I was set on working on a project that was interesting from an engineering point of view, but I also found it important to work on technology that one day could have a positive impact on society. In addition to that, I wanted to obtain more practical experience when it comes to prototyping and I wanted to learn more about testing facilities and equipment that are available at the university. I can honestly say that I did all of the above, which I am very happy with. At the start of my project, there was no clear-cut research objective. By talking with both my supervisor and other students who had worked on topics related to energy harvesting before me, I learned about the interesting challenges that were present within vibration energy harvesting. Slowly but surely, the research objective became more clear and resulted in the research presented in the form of this thesis.

The project was one big learning process. I got to enhance skills such as prototyping, academic writing, problem solving and gained many specific knowledge about vibration energy harvesting. Even though I deem my graduation project to be a success, it also came with failure and disappointment. Learning how to to deal with setbacks and frustration was also part of the learning experience. All those experiences, both the failures and successes, have contributed to a great graduation project.

5.2. RECOMMENDATIONS

First of all, the efficiency of the fabricated prototype presented in Chapter 4 is underestimated due to redundant volume of the metal parts of the prototype. Removing this redundant volume will already make for a lower motion ratio and higher efficiency, without having an effect on the power output. This would give a more realistic view of the performance in comparison to efficiencies reported in literature.

All prototypes fabricated during the graduation project, were on macro scale. The logical next step would be to focus on miniaturization and new production methods that could be used to fabricate a design at this small scale.

Effectively lowering the resonant frequency has shown to be difficult. Nonlinear systems have shown to be effective when it comes to low frequency energy harvesting. It is therefore recommended to focus on non resonant energy harvesters instead of the resonant energy harvesters when it comes to low-frequency operation.

Testing methods should be extended further than the standard frequency sweeps. This research has shown the importance of using a realistic signal, as big differences were seen when comparing the results of when a sine wave was applied to the prototype and when a realistic signal was used, in this case a heartbeat.

When it comes to performing measurements: testing always takes up more time then expected. It is therefore key to pay time and attention to designing and optimizing a test setup right from the start, it will safe you a lot of time and frustrations later on in

the project. Additionally; do not ever think that the measurements you are doing will be your last, this is almost never the case.

5.3. CONCLUSIONS

Energy harvesting is seen as an interesting application in the medical field. An example is a pacemaker, where energy harvesters can take away the need of periodic replacement of the battery. Especially as the power consumption of wearable and implantable devices has gone down, energy harvesters become even more meaningful.

The piezoelectric transducer is popular amongst the energy harvesters, due to their high power density and ease of application. However, the use of off-the-shelf transducers limits the design of the energy harvester. An alternative was offered by proposing both laser cutting and milling as fabrication techniques in order to modify existing piezoelectric diaphragms in order to obtain a desired transducer design. This allowed for more flexibility when it comes to prototyping of energy harvesters.

Both frequency up converters and bistable energy harvesters have been proposed as a solution to the problems that arise for resonating systems. Both were looked into: impact based frequency up converters have been researched in the form of a literature research, resulting in a classification based on the coupling of the low frequency oscillator and high frequency oscillator. A stiffness compensated bistable energy harvester was fabricated and tested for the application in pacemakers. A significant increase in power output was observed when comparing the bistable system to the resonant reference device. It was shown that stiffness compensated bistable energy harvesters show potential to be implemented in medical devices, such as pacemakers, that require low frequency and low force operation.

Also, a significant difference in performance was observed when applying a real heartbeat and when standard sine waves were applied. This shows the importance of using real world excitations for the testing of energy harvesters.

ACKNOWLEDGEMENTS

As my time at TU Delft has come to an end, I can look back at the amazing time I had. I got to meet many incredible people in the form of students, teachers and friends for life. I am very grateful for the opportunities that have been presented to me throughout my years in Delft, which will be something I carry with me for the rest of my life.

First of all, I would like to thank my daily supervisor Thijs Blad for his excellent guidance throughout the project. The times spend on discussions, counselling and monday meetings are very much appreciated. I would also like to thank Peter Steeneken for his enthusiasm, council and the fact that he allowed me to move freely during my project.

Secondly, I would like to thank my fellow group members. Even though a global pandemic got in the way of doing our meetings in real life for most of the year, the useful discussions and point of views have been very helpful throughout the year.

Lastly, I would like to thank my close family and friends who have always supported and motivated me. I want to thank my parents for always being supportive and showing me what it is to work hard. Also, I am lucky to have a great variety of friends with whom I got to share both the happy and the sad parts of life. You really helped me blow off some steam when I needed to, which definitely contributed greatly to the completion of this thesis.

Finally, I would like to thank my partner, Job, for always being there for me and for bringing joy into my life. Thanks for being you, because you are great.

A

PROTOTYPING

During the design of the stiffness compensated bistable energy harvester (SCOBIE), lots of prototypes were fabricated. In this appendix, the evolution of the SCOBIE throughout the project is visualised and elaborated on.

A.1. VERSION 1

The first prototype that was manufactured incorporated packaged-induced preloading, introduced in [46], see Figure A.1a. The flexures-transducer combination (Figure A.1b) is sandwiched between a frame with on one side a gap and the other side an out of plane curve (Figure A.1c), which forces the flexures-transducer combination to follow this curve. This results in shortening of the distance between the flexures and the mass, because of which the flexures start to buckle. This prototype was SLA printed and is thus made of plastic.

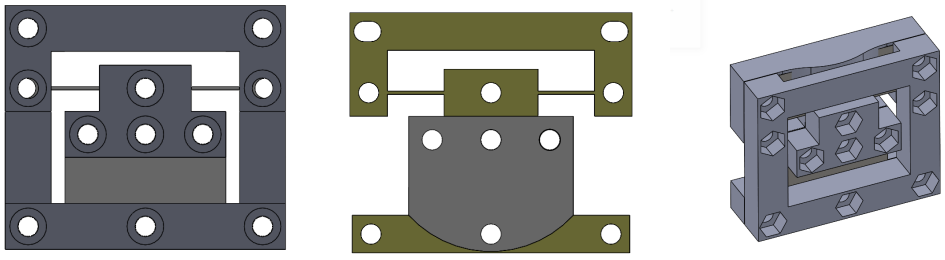

(a) (b) (c)

Figure A.1: a) Prototype using packaged-induced preloading. b) Flexures-transducer combination. c) The thickening in the geometry of the package on the top side makes for a shortening of the flexures, resulting in a preload.

POINTS OF IMPROVEMENT

The preload is dependent on the geometry of the package in this design. After fabrication, the amount of preload is set and can not be changed. However, it is desired to tune the preload after fabrication as well, as this system is very sensitive and therefore might sometimes require some additional or less preload to account for fabrication and assembly errors.

A.2. VERSION 2

For this prototype, the packaged-induced preloading technique was replaced by a tunable preloading technique. The preloading mechanism now consists of two added parallel guidance mechanisms consisting of two pairs of flexures. The masses attached to those flexures are connected by a screw (Figure A.2a). As the screw is tightened, an equal force is exerted on both masses, resulting in a decreasing gap distance between the two masses.This results in a shortening of the metal flexures, because of which they start to buckle. This way, the negative stiffness provided by the flexures is made tunable. As the upper part of the flexures-transducer combination was not necessary anymore, it was removed (Figure A.2b). The base, including the parallel guidance mechanisms, was fabricated by SLA printing.

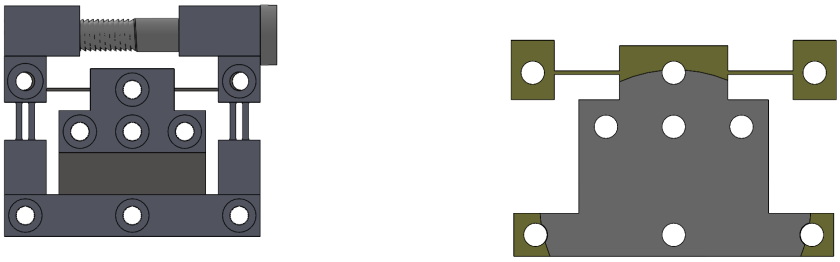

(a) (b)

Figure A.2: a) Tuning mechanism including the set screw. b) Flexures-transducer combination.

POINTS OF IMPROVEMENT

The flexures that form a parallel guidance were put too close together, causing rotations of the masses attached to these flexures. As a horizontal translation is required instead of a rotation, the distance between these flexures should be increased in order counteract the moment acting on the mechanism. The base of the frame started to rotate during preloading as well. Therefore, the base should be made stiffer as well.

A.3. VERSION 3

The distance between the flexures of the parallel guidance mechanisms were set further apart from each other and an extra rib was added to the base of the prototype. The set screw is now sunk into the tuning mechanism.

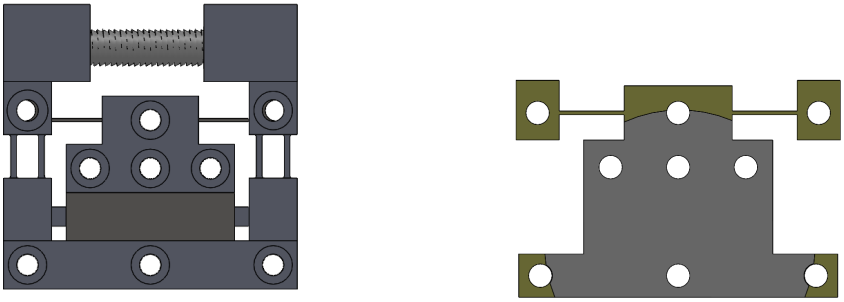

(a) (b)

Figure A.3: a) Tuning mechanism with an added rib and wider flexures in order to reduce unwanted rotations of the frame. b) Flexures-transducer combination.

POINTS OF IMPROVEMENT

Even though quasi-static measurements showed that by tuning the negative stiffness of the flexures using the set screw, the stiffness was effectively changed, there were still a lot of issues. Deformation of both the base and tuning mechanism made for low repeatability (Figure A.4). Also, the stiffnesses of the flexure pairs differed due to inconsistencies caused by 3D printing. This resulted in uneven preloading of the buckled flexures(Figure A.5).

As this was mostly due to inconsistencies in material properties and geometry due to 3D printing, changing the geometry of the mechanism did not seem to solve the issues. Therefore, it was decided that the device should be made out of metal in order to obtain decent repeatability.

Also, the range in which the buckled flexures show approximately linear behaviour, was very small (<1 mm). To obtain a larger range of motion, the length of the flexures should be increased. As this decreases the negative stiffness provided by the flexures, the width of the flexures should be increased as well to compensate for this loss of stiffness.

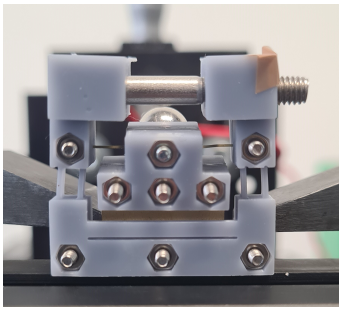

Figure A.4: Undesired deformations were present after preloading.

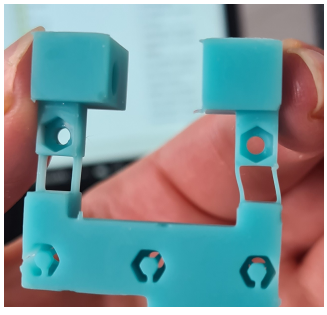

Figure A.5: Different stiffnesses of the flexure pairs resulted in different preloads on the buckled flexures.

A

A.4. FINAL DESIGN

The final design was made out of an aluminum base and preloading blocks (Figure A.6a) as been seen in [43]. The preload of each flexure can be set separately by means of a set screw. Guidance pins make for correct translation of the preloading blocks and prevent rotation. Two additional metal rings were screwed on top of the plastic mass, which has not been depicted in the figure.

Because it was desired to increase both the length and width of the flexures, the flexures-transducer combination was split up into two separate parts, as can be seen in Figure A.6b. This was necessary because the dimensions of the flexures were not going to fit on the piezoelectric diaphragm that was used to fabricate the previous transducer-flexures combinations. The flexures were now fabricated out of 0.1 mm sheet steel.

The problems mentioned before, such as deformation of the frame and poor repeatability, were not present anymore. A picture of the final design can be seen in Figure A.7.

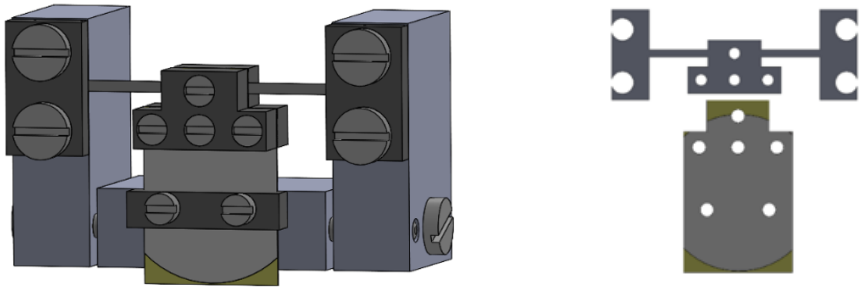

(a) (b)

Figure A.6: a) The final version of the SCOBIE. The plastic frame and tuning mechanism was replaced by an aluminum base and preloading blocks. b) The metal flexures and piezoelectric cantilever.

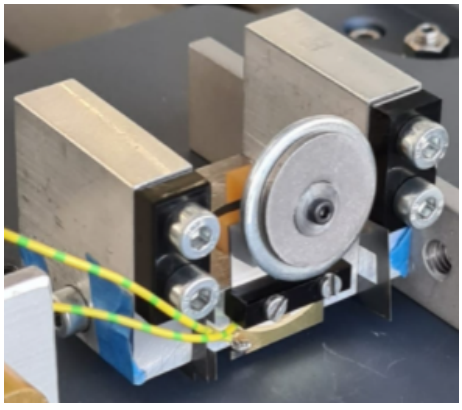

Figure A.7: Assembled prototype with additional masses.

A.5. REFERENCE DEVICE

The non-resonant SCOBIE (Figure A.8a) was compared to a resonant reference device. The buckled flexures were removed, resulting in just the piezoelectric cantilever and proof mass attached to it (Figure A.8b).

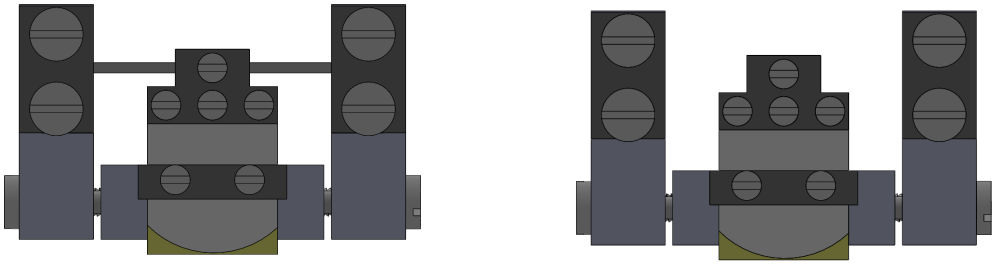

(a) Non-resonant SCOBIE

(b) Resonant reference device.

Figure A.8

B

STIFFNESS TUNING

Force- deflection measurements were performed in order to see whether the stiffness could be tuned successfully using a 3D printed prototype (Version 3, Appendix A). The set screw was tightened, gap distance d was measured and a force deflection measurement was performed using a PI M-505 motion stage, on which a FUTEK LRM200 sensor was mounted, as been described in Chapter 4. The force- deflection curves for the different gap distances can be seen in Figure B.1. It can be seen that for decreasing gap distance and thus increasing preload, the plot starts to rotate clockwise. This indeed shows that the proposed tuning of the stiffness is possible and can be used to obtain the desired characteristics of the system.

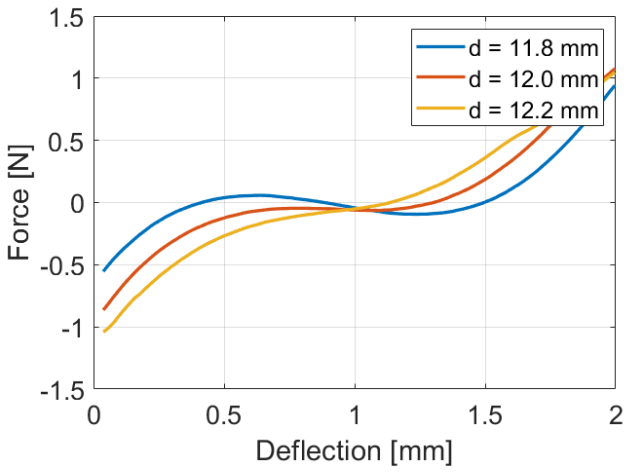

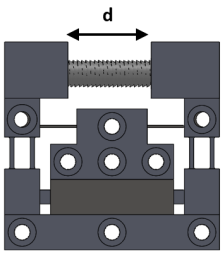

Figure B.1: Results of force- deflection measurements for different gap distances.

C

ZERO STIFFNESS

In the paper presented in Chapter 4, the negative stiffness was tuned in such a way that a bistable system was obtained. However, it can also be used to obtain a stiffness close to zero over a certain range. In case of bistability of the overall system, the negative stiffness provided by the buckled flexures is higher than the positive stiffness of the monostable cantilever. In the case of zero stiffness, the negative stiffness and positive stiffness are equal, resulting in a net stiffness of zero over a given range. This is depicted in Figure C.1, where the negative stiffness (blue) is increased in every subfigure while the linear stiffness (red) stays the same. The black line presents the overall stiffness, with Figure C.1b showing zero stiffness over a certain range. This extremely low stiffness could result in extremely low resonance frequencies, which could be used to harvest energy efficiently at low frequencies.

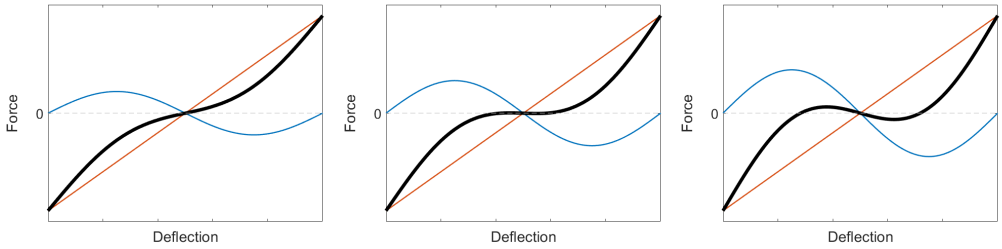

(a) Monostable (b) Zero stiffness (c) Bistable

Figure C.1

By using the tuning mechanism mentioned in Chapter 4 and in Appendix A, the preload was varied in order to obtain zero stiffness. Both quasi-static measurements and dynamic measurements were performed to gain insights in the static characteristics and dynamic behaviour of the statically balanced prototype.

C.1. QUASI-STATIC MEASUREMENTS

Figure C.2 shows the results of a force-deflection measurement. A relatively flat curve can be observed over a range of about 1 mm. In this range, the maximum force measured is below 0.1 N. A hysteresis loop can be observed, caused by the magnetic connection between the mass and the force sensor.

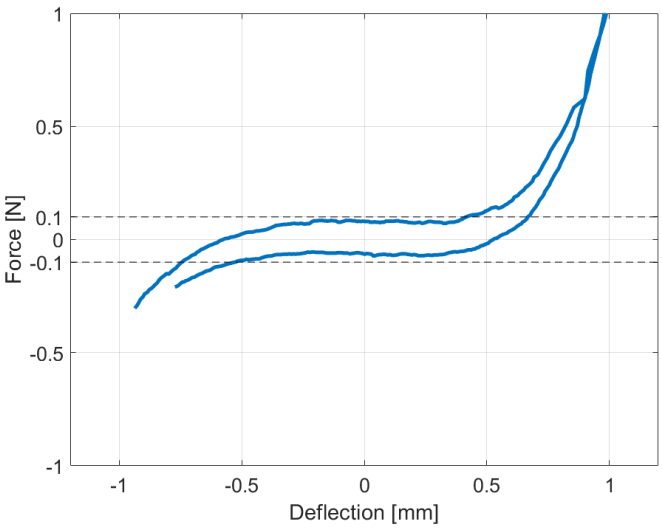

Figure C.2: Force Deflection measurement, showing a nearly horizontal curve over a range of 1 mm. Over this range, the measured force stays below 0.1 N.

C.2. DYNAMIC MEASUREMENTS

Figure C.3 shows the result of frequency sweep, in which the frequency was swept from 30Hz to 1Hz at 0.5g. The device started resonating around 20 Hz, which can also be seen in Figure C.4, where the results of a Fourier analysis can be seen. A maximum amplitude can be observed around 20 Hz. The resonance frequency of the cantilever without buckled flexures was experimentally determined to be around 30 Hz, which is talked about in more detail in Appendix G. This means that the stiffness compensation resulted in a 30% decrease in natural frequency.

Even though a decrease of 30% shows that using negative stiffness as a way to obtain lower natural frequencies is effective, it still does not provide a low enough natural frequency in order to obtain high efficiency for frequencies below 10 Hz. The mechanism is very sensitive, so to correctly tune the mechanism to actually obtain zero stiffness and to obtain an extremely low natural frequency, is really difficult. Fabrication errors and assembly errors can already have a great influence on the performance, which is probably the reason why the lowest natural frequency that was obtained was just 20 Hz.

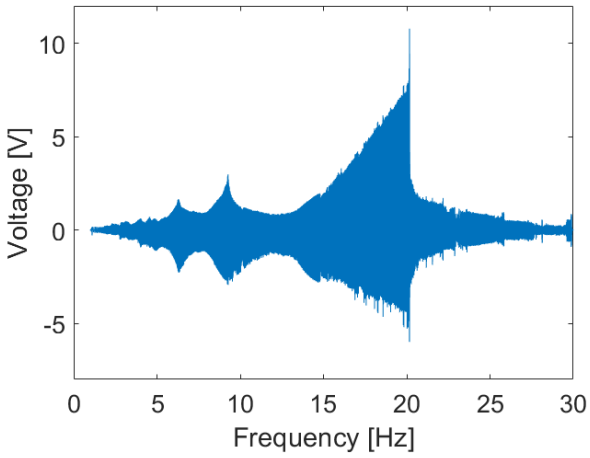

Figure C.3: Voltage output for a frequency sweep (downwards) from 30 to 1 Hz at 0.5g with a duration of 300 seconds.

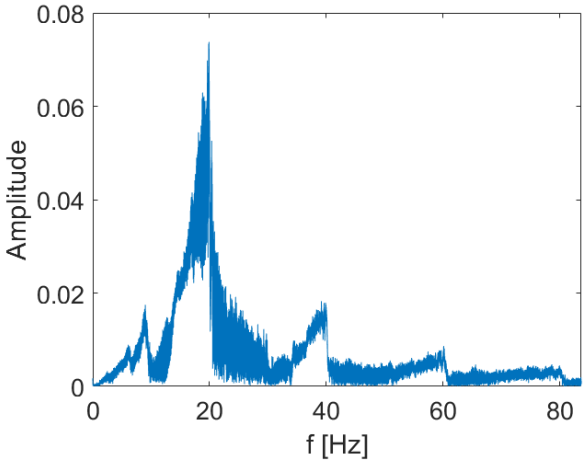

Figure C.4: FFT analysis of the voltage output presented in Figure C.3.

C.3. CONCLUSION

The results show that using stiffness compensation as a way to lower the resonance frequency, is successful. However, due to the sensitivity of the system, it is difficult to actually obtain resonance at low frequency (<10 Hz). In order to successfully lower the resonance to extremely low frequencies, mainly fabrication errors and assembly errors should be reduced. Because a bistable mechanism made for high power output for frequencies below 10 Hz as well, it was decided to focus on obtaining a low stiffness bistable system.

D

Optimal Load

For every operating frequency an optimal load can be defined which maximizes the power output for these conditions. Even though the operating frequency is not constant, a good conception of the order of magnitude will help already. Because in this case the transducer has been laser cut out of piezoelectric element in a certain shape and the material properties of the piezoelectric ceramic of the element are unknown, the optimal load was determined by means of a practical experiment. A 20 Hz sinusoidal wave at 0.5 g was applied to the energy harvester by a linear motor stage (Figure D.1). A variable resistor was used in order to change the resistance over a period of time (Figure D.2). During operation, the resistance was increased every 5 seconds. The voltage and power output over time can be seen in Figure D.3. The voltage output increased with increasing resistance as expected, but the power output shows a clear optimum. The power output versus resistance can be seen in Figure D.4. Under the given conditions, the power output showed an optimum at 100 kOhm. Therefore, this has been chosen as the order of magnitude for all experiments that were performed throughout this graduation project.

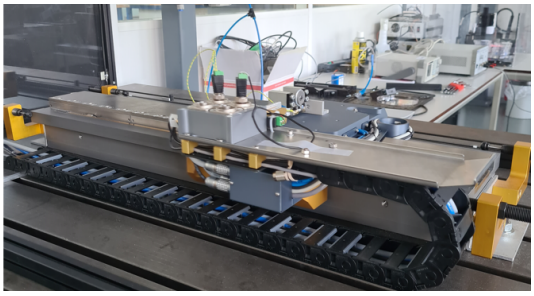

Figure D.1: Motion stage used for the measurement.

Figure D.2: The variable resistance.

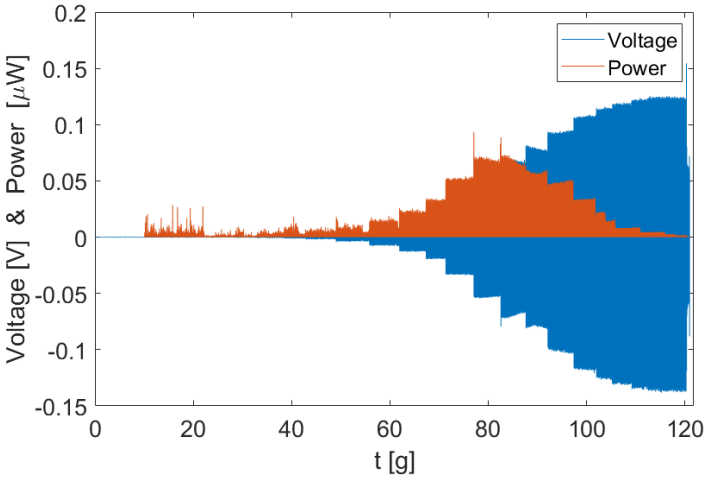

Figure D.3: Voltage output and Power at 20 Hz and 0.5 g. During the measurements the resistance was increased every 5 seconds.

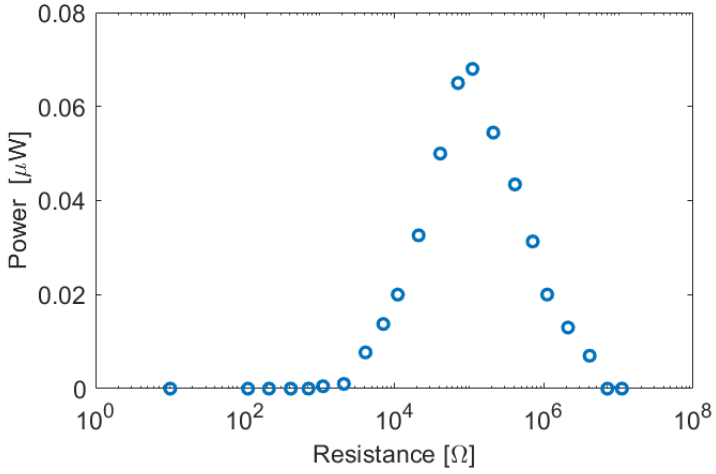

Figure D.4: Power output for varying loads. A maximum power output is observed at 100 kOhm.

E

STEP-BY-STEP: ASSEMBLY AND DYNAMIC TESTING

E.1. ASSEMBLY

1. Start out with clamping the piezoelectric cantilever to the base using the clamping block and two screws.
2. Sandwich the flexures and cantilever between the two plastic parts of the mass. Do not attach the heavier circular masses yet.
3. Position the pre-loading blocks in such a way that when the flexures are attached to them, they won't be preloaded. Attach the flexures to the preloading blocks, using the two clamping blocks and screws.
4. Fill the space between the base and pre-loading blocks with spacers.
5. Remove the upper screw of the mass, replace it by a longer one and use it to now add the heavier metal disks to the plastic mass.
6. Perform a continuity test using a multimeter. Sometimes the screws that are used to attach the cantilever to the base, make contact with the silver electrode on top of the ceramic. If so, unscrew and tighten these bolts until continuity is removed.
7. Tighten both set screws.
8. Remove spacers and tighten set screw until desired stiffness is obtained.
9. Check whether the acceleration threshold is lower than 1g by rotating the device slowly around its horizontal axis and see whether snap through motion is induced. If not, go back to step 7.
10. If the threshold acceleration is lower than 1g, the prototype is ready to be attached to the motion stage. Further tuning will be done in between the measurements.

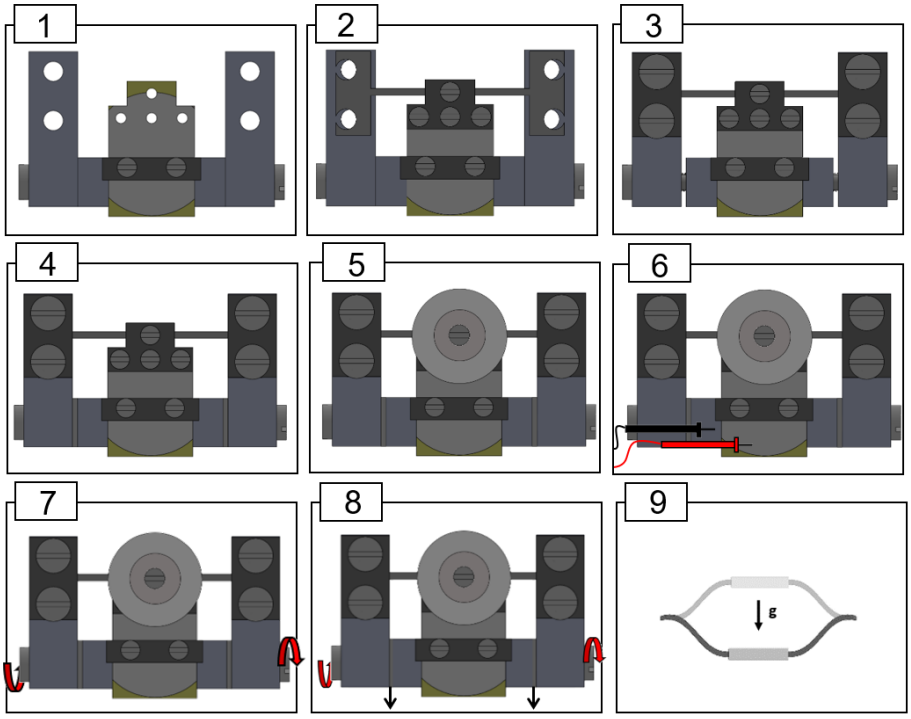

Figure E.1: Visualisation of the different assembly steps.

E.2. DYNAMIC TESTING

NOTE: This is not instruction on how to use the motion stage and corresponding software properly. For that information you are referred to the instruction manual of the linear motion stage.

1. Start up motion stage and software as described in the instruction manual.
2. Make sure to measure over a resistance in the order of magnitude of 100 kOhm.
3. Perform an acceleration sweep from 0.1g tot 2g. Plot the voltage output vs. acceleration. A sudden increase in voltage output shows the threshold acceleration that is required for snap through behaviour.
4. If the desired threshold acceleration is not obtained yet, tune the prototype using the set screws and repeat step 3.
5. Start with testing.
6. After performing a couple of measurements, go back to step 3 to check whether the the threshold acceleration has changed. This might happen when sharp acceleration changes are present in a signal.
7. Shut down motion stage and software as described in the instruction manual.

F

PIEZOELECTRIC COMPOSITE SAMPLE

One of the most popular piezoelectric materials is lead zirconate titanate (PZT) due to high piezoelectric constants. However, these ceramics are also stiff and brittle. Especially for energy harvesting at low frequency, high stiffness and thus high natural frequencies are a problem. The more flexible piezoelectric polymers such as PVDF usually make for a poor power output, as they contain lower piezoelectric constants. Research is conducted by the faculty of Aerospace at TU Delft into polymer-piezoceramic composites [47]. A polymer matrix provides the flexibility, while a ceramic filler provides the piezoelectric properties. This was explored as one of the options which could be used for the eventual prototyping.

Tadhg Mahon, who is currently doing his postdoc at the faculty of aerospace, provided a sample of a piezoelectric composite made of piezoceramic power and a polymer matrix. Together we decided on which volume fraction would be most suitable for the type of loading. A picture and a close up of the sample can be seen in Figure F.1a and F.1b . Unfortunately, as the sample was provided relatively late into the graduation project, it was too late to actually use and test the sample that was provided.

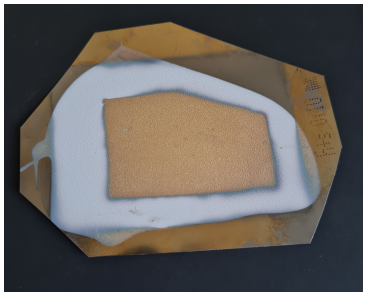

(a) Piezoelectric composite sample

(b) Close up of the sample

G

OTHER RELEVANT MEASUREMENTS

G.1. NATURAL FREQUENCY DETERMINATION

In order to experimentally determine the natural frequency of the piezoelectric cantilever, the voltage output was measured when striking the cantilever. The results of this experiment can be seen in Figure G.1. A ring-down is observed, from which the natural frequency of the cantilever can be determined. A Fourier analysis was performed (Figure G.2), from which it can be concluded that the natural frequency of the cantilever, without negative stiffness added to it, is about 30 Hz.

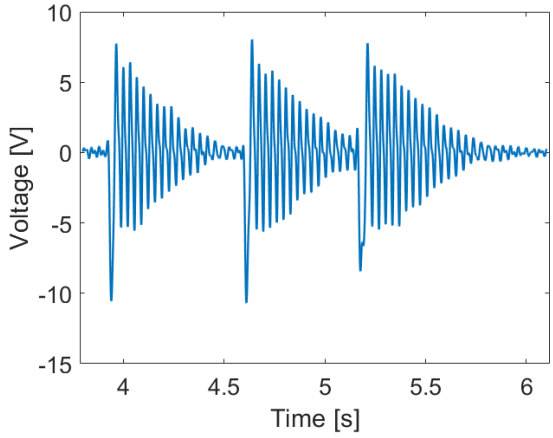

Figure G.1: Voltage output for a frequency sweep (downwards) from 30 to 1 Hz at 0.5g with a duration of 300 seconds.

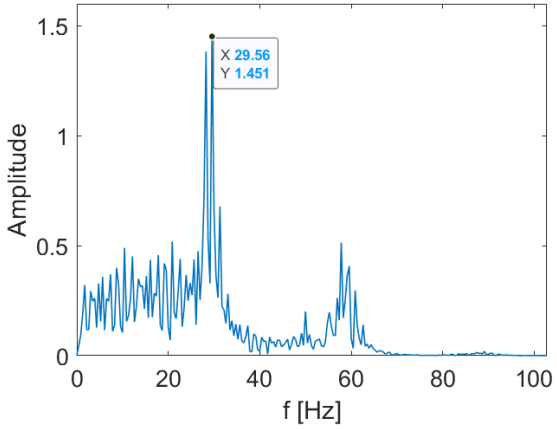

Figure G.2: FFT analysis of the voltage output presented in Figure G.1.

G.2. MEASUREMENT AT THRESHOLD ACCELERATION ($a = 0.4g$)

An acceleration sweep performed from 0.1g to 2g for a constant frequency of 2 Hz was shown in the paper presented in Chapter 4 and can again be seen in Figure G.3. A threshold acceleration of 0.4g was obtained, which can be recognized by the sudden in crease in voltage output.

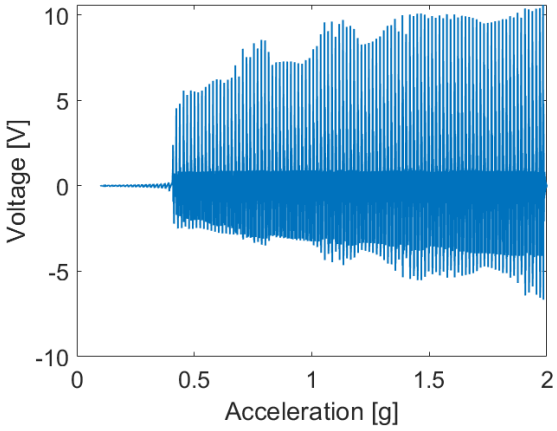

Figure G.3: Acceleration sweep from 0.1g to 2g at 2Hz.

Measurements were performed at approximately the threshold acceleration of 0.4g at a frequency of 1Hz. The results can be seen in Figure G.4. What can be seen is that the snap through motion is induced for a while, but at some point stops. This shows that 0.4g is very close to the threshold acceleration, as the system seems to balance between operational and not operational for the acceleration of 0.4g.

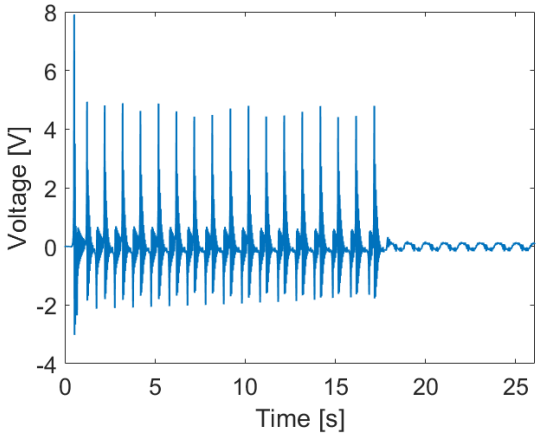

Figure G.4: Voltage output for a sine wave at 0.4g and 1Hz.

G.3. MEASUREMENT PERFORMED AT LOWEST FREQUENCY AND ACCELERATION.

Because 0.4g has shown to be balancing between operational and not operational, a measurements was performed at an acceleration of 0.5g and at 0.75 Hz. The results can be seen in Figure G.5 and show that during the entire measurement of 30 seconds, snap through motion was induced. An average power output of 2.7μW was measured, making for an efficiency of 0.04% and a motion ratio of 0.068.

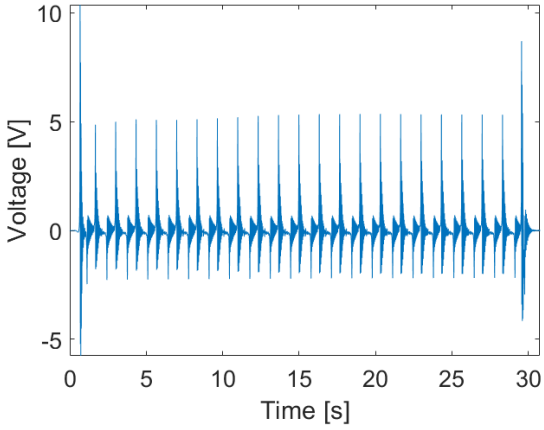

Figure G.5: Voltage output for a sine wave at 0.5g and 0.75Hz.

H

IMPACT BASED FREQUENCY-UP CONVERTER

H.1. INTRODUCTION

Frequency up-converters have been proposed as solution for the inefficient energy harvesting for low frequency and large amplitude motions. These frequency up-converters consists of a low frequency oscillators that activates a high frequency oscillator, causing the low frequency oscillation to be up conversed into a high frequency motion. In this appendix an impact based frequency up-converter design is shown.

H.2. DESIGN

H.2.1. LITERATURE REVIEW

Prior to writing the literature review about impact driven frequency up-converters presented in Chapter 2, I made an overview in which I sketched the designs that I found in literature in the form of mass-spring systems. These sketches can be seen in Figure H.1 and H.2. I was able to distinguish two types of frequency up-converters: designs in which the low frequency oscillator and high frequency oscillator are stacked on top of each other. As the low frequency oscillator makes an impact, the high frequency oscillator gets an impulse like response and starts to vibrate. The other group are designs in which the low frequency oscillator directly impacts the high frequency oscillator. Those were referred to as stacking type and hammer type frequency up-converters, which is proposed as a way to classify impact driven frequency up-converters in the literature research that was presented.

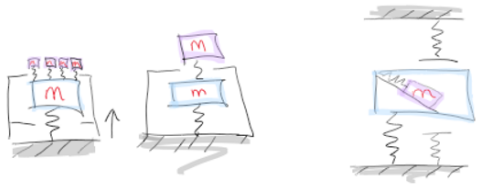

Figure H.1: Stacking type frequency up-converters.

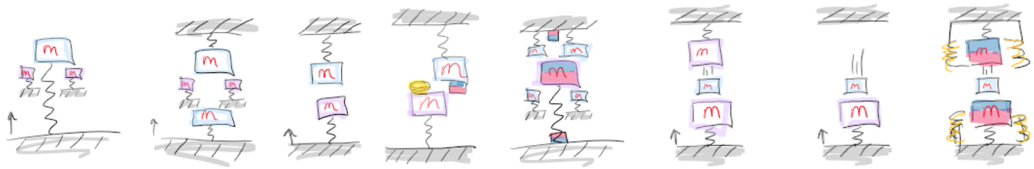

Figure H.2: Hammer type frequency up-converters.

H.2.2. BRAINSTORM

It was decided to do a brainstorm for both the low frequency oscillator and high frequency oscillator design separately. Afterwards, ideas for the low frequency oscillator and high frequency oscillator were combined into a complete frequency up-converter design. The results can be seen in Figure H.3.

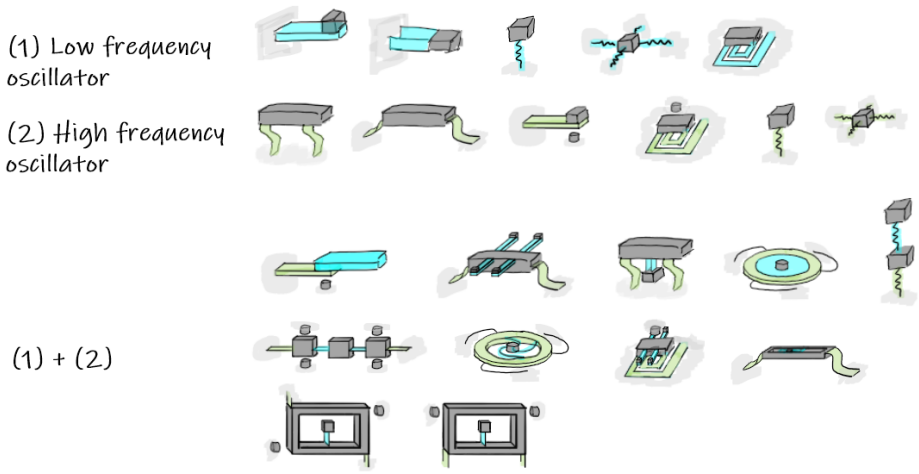

Figure H.3: Results of a brainstorm session.

As I found it important to start quickly with prototyping in order to get more experienced with this process, I decided to go for a design which would be relatively easy to fabricate and assemble. Therefore, it was decided to go for a stacking type frequency up-converter which in its most simple form is similar to the system depicted below.

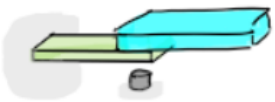

Figure H.4

H.2.3. DESIGN DETAILS

The frequency up-converter that was manufactured, consists of an aluminum base with a parallel guidance made of two steel sheets clamped within the base, see Figure H.5a and H.5b. The length of the parallel guidance is adjustable, so different stiffnesses (eq. H.1) can be obtained depending on the effective length L_{eff} of the steel sheets. Important parameters of the steel flexures can be found in Table H.1. A 3D printed frame is clamped between the ends of the parallel guidance, with a piezoelectric cantilever taped on top of the frame. The piezoelectric cantilever is made out of a piezoelectric diaphragm (KEPO FT-41T) and is laser cut into the desired shape, which presents the high frequency oscillator. Two leads are soldered onto the high frequency oscillator. A set screw is screwed into the base, with which the low frequency oscillator will collide after a certain gap distance d_g is bridged by the low frequency oscillator, which can be set with the set screw. As the low frequency oscillator impacts the set screw, the high frequency oscillator will start to vibrate in its natural frequency.

$$k_1 = k_2 = \frac{3EI}{L_{eff}^3} \quad k_{LFO} = k_1 + k_2 \tag{H.1}$$

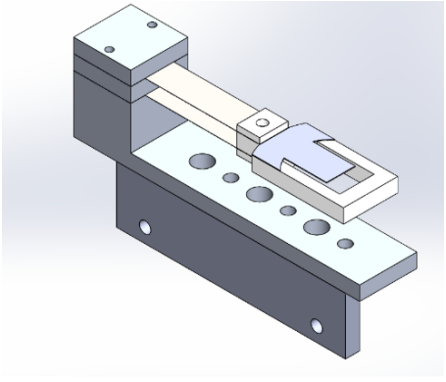

(a)

(b)

Figure H.5: a) 3D model of the proposed frequency up-converter. b) Picture of manufactured frequency up-converter.

Parameter	Symbol	Value
Flexure Width	W_f	10 mm
Flexure Length	L_{eff}	Var
Flexure Thickness	t_f	0.1 mm
Young's Modulus	E_f	200 GPa
Density	ρ_f	8050 kg/m^3

Table H.1: Parameters of the steel flexures.

H.3. CONCLUSION

The fabrication of the frequency up-converter presented in this Appendix, was the first actual energy harvester that was build as a part of this graduation project. It was never actually properly used and tested, as during the project other type of energy harvesters seemed more interesting. However, the designing and manufacturing of this frequency up-converter provided practical experience, which was used throughout the rest of the project.

BIBLIOGRAPHY

[1] P. D. Paulo J.and Gaspar, "Review and future trend of energy harvesting methods for portable medical devices," *WCE 2010 - World Congress on Engineering 2010*, vol. 2, 2010.

[2] A. Erturk and D. J. Inman, *Piezoelectric energy harvesting*. John Wiley Sons, 2011.

[3] K. Cook-Chennault, N. Thambi, M. A. Bitetto, and E. Hameyie, "Piezoelectric energy harvesting," *Bulletin of Science, Technology Society*, vol. 28, 2008.

[4] E. Dechant, F. Fedulov, D. V. Chashin, L. Y. Fetisov, Y. K. Fetisov, and M. Shamonin, "Low-frequency, broadband vibration energy harvester using coupled oscillators and frequency up-conversion by mechanical stoppers," *Smart Materials and Structures*, vol. 26, 2017.

[5] T. W. Blad and N. Tolou, "On the efficiency of energy harvesters: A classification of dynamics in miniaturized generators under low-frequency excitation," *Journal of Intelligent Material Systems and Structures*, vol. 30, 2019.

[6] G. Chen and E. Rodriquez-Villegas, "Harvesting energy from the motion of human limbs: The design and analysis of an impact-based piezoelectric generator," *System-level design trade-offs for truly wearable wireless medical devices*, 2010.

[7] T. W. A. Blad, J. H. D. Farhadi Machekposhti, A. Holmes, and N. Tolou, "Vibration energy harvesting from multi-directional motion sources," *MARSS 2018 - International Conference on Manipulation, Automation and Robotics at Small Scales*, 2018.

[8] B. Maamer, A. Boughamouora, A. M. R. F. El-Bab, L. Francis, and F. Tounsi, "A review on design improvements and techniques for mechanical energy harvesting using piezoelectric and electromagnetic schemes," *Energy Conversion and Management*, vol. 199, 2019.

[9] A. R. M. Siddique, S. Mahmud, and B. V. Heyst, "A comprehensive review on vibration based micro power generators using electromagnetic and piezoelectric transducer mechanisms," *Energy Conversion and Management*, vol. 106, 2015.

[10] L. Gu and C. Livermore, "Impact-driven, frequency up-converting coupled vibration energy harvesting device for low frequency operation," *Smart Materials and Structures*, vol. 20, 2011.

[11] M. A. Halim, S. Khym, and J. Y. Park, "Frequency up-converted wide bandwidth piezoelectric energy harvester using mechanical impact," *Journal of Applied Physics*, vol. 114, 2013.

[12] C. Wang, Q. Zhang, and W. Wang, "Low-frequency wideband vibration energy harvesting by using frequency up-conversion and quin-stable nonlinearity," *Smart Materials and Structures*, vol. 399, 2017.

[13] R. Dauksevicius, D. Briand, R. Lockhart, A. V. Quintero, N. de Rooij, R. Gaidys, and V. Ostasevicius, "Frequency up-converting vibration energy harvester with multiple impacting beams for enhanced wideband operation at low frequencies," *Procedia Engineering*, vol. 87, 2014.

[14] S Jung and K. Yun, "Energy-harvesting device with mechanical frequency-up conversion mechanism for increased power efficiency and wideband operation," *Applied Physics Letters*, vol. 96, no. 11, pp. 94–97, 2010.

[15] K. Ashraf, M. H. M. Khir, and Z. Baharudin, "Improved energy harvesting from low frequency amplification at multiple frequencies.," *Sensors and Actuators A: Physical*, vol. 195, 2013.

[16] P. D. Mitcheson, E. M. Yeatman, G. K. Rao, A. S. Holmes, and T. C. Green, "Human and machine motion for wireless electronic devices," *Proceeding of the IEEE*, vol. 96, 2008.

[17] H. Liu, C. Lee, T. Kobayashi, C. J. Tay, and C. Quan, "Investigation of a mems piezoelectric energy harvester system with a frequency-widened-bandwidth mechanism introduced by mechanical stoppers," *Smart Materials and Structures*, vol. 21, 2012.

[18] Zorlu, E. Topal, and H. Külah, "A vibration-based electromagnetic energy harvester using mechanical frequency up-conversion method," *IEEE Sensors Journal*, vol. 11, 2011.

[19] R. Lensvelt, R. Fey, R. Mestrom, and H. Nijmeijer, "Design and numerical analysis of an electrostatic energy harvester with impact for frequency up-conversion," *Journal of Computational and Nonlinear Dynamics*, vol. 15, 2020.

[20] S. Roundy and Y. Zhang, "Toward self-tuning adaptive vibration-based microgenerators," *Proc. SPIE, Smart Structures, Devices, and Systems II,*, vol. 5649, 2005.

[21] M. Renaud, P. Fiorini, R. Van Schaijk, and C. Van Hoof, "Erratum: Harvesting energy from the motion of human limbs: The design and analysis of an impact-based piezoelectric generator," *Smart Materials and Structures*, vol. 18, 2009.

[22] S. Liu, Q. Cheng, D. Zhao, and L. F. Harbin, "Theoretical modeling and analysis of two-degree-of-freedom piezoelectric energy harvester with stopper," *Sensors and Actuators A: Physical*, vol. 245, 2016.

[23] M. Halim and J. Park, "Piezoelectric energy harvester using impact-driven flexible side-walls for human-limb motion," *Microsystem Technologies*, vol. 24, 2017.

[24] T. W. A. Blad, J. H. D. Farhadi Machekposhti, A. Holmes, and N. Tolou, "Design of a motion energy harvester based on compliant mechanisms: A bi-stable frequency up-converter generator," *Advances in Mechanism and Machine Science*, vol. 73, 2019.

[25] V. Rouillard, "Excitation techniques for resonance analysis of packages," *Packaging Technology and Science*, vol. 15, 2002.

[26] R. B. van Kempen, "Monolithic piezoelectric vibration energy harvesting," Master's Thesis, Technical University Delft, XXX, 2016.

H

[27] S. Nadig, S. Ardanuc, and A. Lal, "Planar laser-micro machined bulk pzt bimorph for in-plane actuation," *2013 Joint IEEE International Symposium on Applications of Ferroelectric and Workshop on Piezoresponse Force Microscopy*, 2013.

[28] F. S. Huang, Z. H. Feng, Y. T. Ma, Q. S. Pan, L. S. Zhang, Y. B. Liu, and L. G. He, "High-frequency performance for a spiral-shaped piezoelectric bimorph," *Modern Physics Letters B*, 2018.

[29] N. T. Jafferis, M. J. Smith, and R. J. Wood, "Design and manufacturing rules for maximizing the performance of polycrystalline piezoelectric bending actuators," *Modern Physics Letters B*, vol. 24, p. 6, 2015.

[30] T. W. A. Blad, N. Tolou, R. A. J. van Ostayen, and J. L. Herder, "Statically balanced compliant ortho-planar mechanism for extremely low-frequency energy harvesting," *PrePrint*, 2021.

[31] A. Zurbuchen, A. Pfenniger, A. Stahel, C. T. Stoeck, S. Vandenberghe, M Koch, and R. Vogel, "Energy harvesting from the beating heart by a mass imbalance oscillation generator," *Annals of Biomedical Engineering*, vol. 7, pp. 131–141, 2013.

[32] J. Chen, H. Chang, and Y. Liu, "Micro-piezoelectric pulse diagnoser and frequency domain analysis of human pulse signals," *Journal of Traditional Chinese Medical Sciences*, 2018.

[33] S.-G. Kim, S. Priya, and I. Kanno, "Piezoelectric mems for energy harvesting," *MRS Bulletin*, vol. 37, pp. 1039–1050, 2012.

[34] W. Q. Liu, A. Badel, F. Formosa, and A. Wu Y. P.; Agbossou, "Novel piezoelectric bistable oscillator architecture for wideband vibration energy harvesting," *Smart Materials and Structures*, vol. 22, no. 3, pp. 1039–1050, 2013.

[35] A. Erturk and N. Elvin, *Advances in Energy Harvesting Methods*. Springer, 2013.

[36] F. Cottone, V. H. Gammaitoni L., M. Ferrari, and V. Ferrari, "Piezoelectric buckled beams for random vibration energy harvesting," *Smart Materials and Structures*, vol. 21, 2012.

[37] M. H. Ansari and M. Karami, "A sub-cc nonlinear piezoelectric energy harvester for powering leadless pacemakers," *Journal of Intelligent Material Systems and Structures*, vol. 29, no. 3, pp. 438–445, 2018.

[38] B. Ando, S. Baglio, A. R. Bulsara, V. Marletta, I. Medico, and S. Medico, "A double piezo - snap through buckling device for energy harvesting," *Transducers and Eurosensors XXVII: The 17th International Conference on Solid-State Sensors, Actuators and Microsystems, TRANSDUCERS and EUROSENSORS 2013*, pp. 43–45, 2013.

[39] E. van de Wetering, T. Blad, and R. van Ostayen, "A stiffness compensated piezoelectric energy harvester for low-frequency excitation," *Smart Materials and Structures*, p. 30, 2021.

[40] H. X. Zou, W. M. Zhang, W. B. Li, K. X. Wei, K. M. Hu, Z. K. Peng, and Z. K. Peng, "Magnetically coupled flextensional transducer for wideband vibration energy harvesting: Design, modeling and experiments," *Journal of Sound and Vibration*, vol. 416, pp. 55–79, 2018.

[41] M. Ferrari, V. Ferrari, M. Guizzetti, M. Guizzetti, B. Andò, S. Baglio, and C. Trigona, "Improved energy harvesting from wideband vibrations by nonlinear piezoelectric converters," *Sensors and Actuators, A: Physical*, vol. 162, no. 2, pp. 425–431, 2010.

[42] M. F. Dempsey, B. Condon, and D. M. Hadley, "Mri safety review," *Elsevier Science*, vol. 23, no. 5, pp. 392–401, 2002.

[43] T. W. A. Blad, N. Tolou, and R. A. J. van Ostayen, "A method for tuning the stiffness of building blocks for statically balanced compliant ortho-planar mechanisms," *Mechanism and Machine Theory*, vol. 162, 2021.

[44] R. Bastiaanse, J. Roos, T. W. A. Blad, N. Tolou, and J. W. Spronck, "Combining cardiac measurement techniques to improve testing for energy harvesting pacemakers," *Master Thesis, TU Delft*, 2021.

[45] P. Pillatsch, E. Yeatman, and A. Holmes, "A scalable piezoelectric impulse-excited energy," vol. 21, 2012.

[46] M. Mariello, T. W. A. Blad, M. Mastronardi, F. Guido, N. Staufer, N. Tolou, R. A. J. van Ostayen, and J. L. Herder, "Flexible piezoelectric aln transducers buckled through package-induced preloading for mechanical energy harvesting," *Nano Energy*, vol. 85, 2021.

[47] V. L. Stuber, T. R. Mahon, S. Van Der Zwaag, and P. Groen, "The effect of the intrinsic electrical matrix conductivity on the piezoelectric charge constant of piezoelectric composites," *Materials Research Express*, vol. 7, 2019.